



FE27294

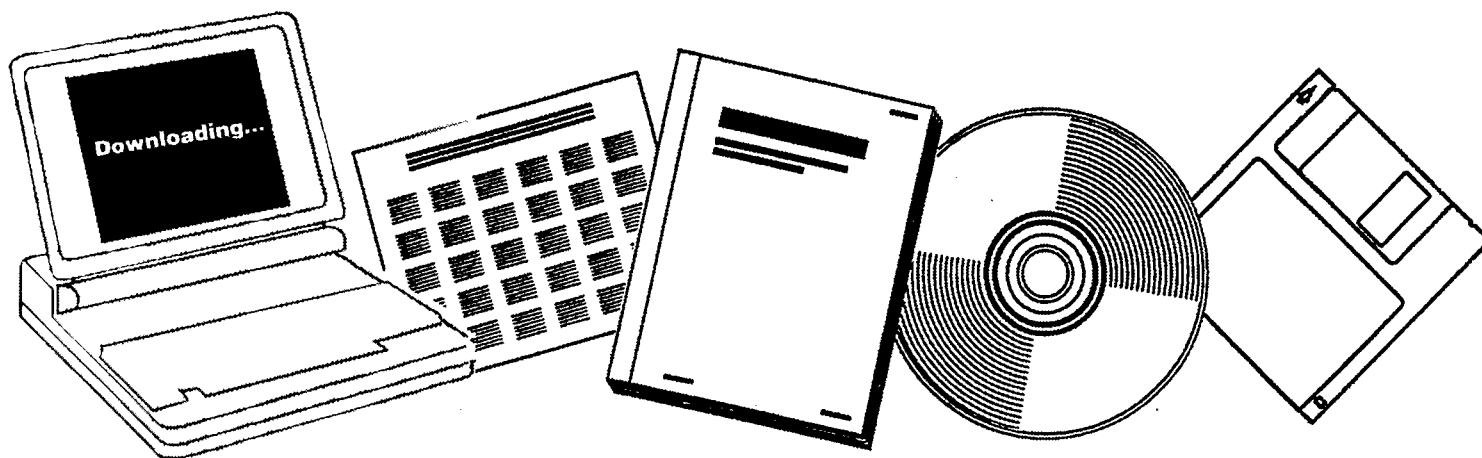
**NTIS**

One Source. One Search. One Solution.

**ALLOY CATALYSTS WITH MONOLITH SUPPORTS FOR  
METHANATION OF COAL-DERIVED GASES. ANNUAL  
TECHNICAL PROGRESS REPOT, SEPTEMBER 20,  
1977--SEPTEMBER 20, 1978**

BRIGHAM YOUNG UNIV.  
PROVO, UT

OCT 1978



U.S. Department of Commerce  
**National Technical Information Service**

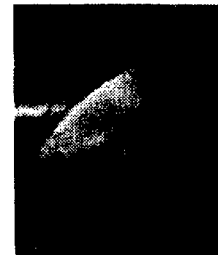
**One Source. One Search. One Solution.**

# NTIS



## **Providing Permanent, Easy Access to U.S. Government Information**

National Technical Information Service is the nation's largest repository and disseminator of government-initiated scientific, technical, engineering, and related business information. The NTIS collection includes almost 3,000,000 information products in a variety of formats: electronic download, online access, CD-ROM, magnetic tape, diskette, multimedia, microfiche and paper.



### **Search the NTIS Database from 1990 forward**

NTIS has upgraded its bibliographic database system and has made all entries since 1990 searchable on **www.ntis.gov**. You now have access to information on more than 600,000 government research information products from this web site.

### **Link to Full Text Documents at Government Web Sites**

Because many Government agencies have their most recent reports available on their own web site, we have added links directly to these reports. When available, you will see a link on the right side of the bibliographic screen.

### **Download Publications (1997 - Present)**

NTIS can now provides the full text of reports as downloadable PDF files. This means that when an agency stops maintaining a report on the web, NTIS will offer a downloadable version. There is a nominal fee for each download for most publications.

For more information visit our website:

**www.ntis.gov**



U.S. DEPARTMENT OF COMMERCE  
Technology Administration  
National Technical Information Service  
Springfield, VA 22161

FE27294



ALLOY CATALYSTS WITH MONOLITH SUPPORTS FOR  
METHANATION OF COAL-DERIVED GASES

Annual Technical Progress Report  
For Period September 20, 1977 to September 20, 1978

Calvin H. Bartholomew  
Brigham Young University  
Provo, Utah 84602

Date Published -- October 5, 1978

PREPARED FOR THE UNITED STATES  
DEPARTMENT OF ENERGY

Under Contract No. EF-77-S-01-2729

## FOREWORD

This report summarizes technical progress during the first year (September 20, 1977 to September 20, 1978) of a two-year study conducted for the Department of Energy (DOE) under Contract No. EF-77-S-01-2729. The principal investigator for this work was Dr. Calvin H. Bartholomew; Dr. Paul Scott was the technical representative for DOE.

The following students contributed to the technical accomplishments and to this report: Graduates - Erek Erekson, Ed Sughrue, and Gordon Weatherbee, and Undergraduates - Kevin Mayo, Don Mustard, and John Watkins. April Barndollar and Steve Kvalve provided typing and drafting services. The assistance of Dr. Phil Reucroft of the University of Kentucky in providing x-ray data is gratefully acknowledged. In this report data are reported in SI units.

## TABLE OF CONTENTS

FOREWORD . . . . .	ii
LIST OF TABLES . . . . .	iv
LIST OF FIGURES . . . . .	v
ABSTRACT . . . . .	1
I. OBJECTIVES AND SCOPE . . . . .	2
A. Background . . . . .	2
B. Objectives . . . . .	2
C. Technical Approach . . . . .	3
II. SUMMARY OF PROGRESS . . . . .	7
III. DETAILED DESCRIPTION OF TECHNICAL PROGRESS . . . . .	11
IV. CONCLUSIONS . . . . .	59
V. REFERENCES . . . . .	61

## LIST OF TABLES

1. Description of Reactor Tests for Task 2 . . . . .	5
2. Catalyst Codes and Compositions . . . . .	12
3. Summary of Metal Surface Area Measurements Using H <sub>2</sub> Chemisorption at 25°C . . . . .	13
4. Carbon Analysis of Catalyst Samples . . . . .	16
5. Comparison of Carbon Monoxide and Hydrogen Chemisorption Measure- ments on 3% Nickel on Alumina Powdered Catalyst . . . . .	17
5A. Comparison of Particle Sizes Calculated from X-ray Line Broadening Hydrogen Adsorption and Electron Microscopy . . . . .	19
6. Results of Carbon Deposition Tests of Monolithic Supported Nickel and Nickel Bimetallic Catalysts . . . . .	26
7. Effects of In Situ H <sub>2</sub> S Poisoning on Activity of Powdered Alumina- Supported Nickel and Nickel Bimetallics at 523K . . . . .	29
8. Effects of In Situ Poisoning on the Activities of Nickel Bimetallic Monolithic Catalysts with 10 ppm H <sub>2</sub> S at 523K . . . . .	32
9. Differential Reactor Data for Ni-Co-A-100 Before and After H <sub>2</sub> S Poisoning . . . . .	34
10. Specific Activity Data Before and After Exposure to 10 ppm H <sub>2</sub> S of Alumina-Supported Ni, Ni-Co and Co in Powder Form . . . . .	37
11. Temperature Conversion Tests for Monolithic Catalysts, GHSV = 30,000 hr <sup>-1</sup> , Reactant Composition: 95% N <sub>2</sub> , 4% H <sub>2</sub> , 1% CO; 140 kPa .	39
12. Comparison of Geometrical Surface Area and Reaction Rates . . . . .	41
13. Experimental and Theoretical Mass Transfer Coefficients . . . . .	43
14. Comparison of Geometrical Surface Area and Reaction Rates . . . . .	44
15. Comparison of Geometrical Surface Area and Conversion Production and Selectivity . . . . .	45

## LIST OF FIGURES

1. Project Progress Summary . . . . .	8
2. Particle size distribution of Ni-A-119 before sintering . . . . .	20
3. Particle size distribution of Ni-A-119 after sintering . . . . .	21
4. Electron micrograph of BL-A-101 (blank alumina support) 295,000x . . . . .	22
5. Electron micrograph of Ni-A-121 (6% Ni) 295,000x . . . . .	23
6. Activity versus Time during Carbon Deposition Tests for Various Monolithic Catalysts . . . . .	25
7. Smoothed Activity-Time Curves for Powdered Alumina-supported Nickel and Nickel Bimetallics during Exposure to 10 ppm H <sub>2</sub> S in 1% CO, 4% H <sub>2</sub> , and 95% N <sub>2</sub> . . . . .	28
8. Activity normalized to hydrogen uptake versus time during reaction at 525K, 110 kPa, and 30,000 hr <sup>-1</sup> . Reaction mixture = 99% H <sub>2</sub> , 1% CO, 10 ppm H <sub>2</sub> S . . . . .	30
9. Smoothed Activity-Time Curves for Monolithic-supported nickel and nickel Bimetallics during Exposure to 10 ppm in 1% CO, 4% H <sub>2</sub> , and 95% N <sub>2</sub> . . . . .	33
10. Fluidized Bed Reactor . . . . .	36
11. Conversion vs. temperature for Ni-AM-201 . . . . .	40
12. CO conversion vs. Temperature for Ni-M-156 and Ni-A-121 . . . . .	47
13. Conversion of CO (overall) vs. Temperature for High Loading Catalysts at 2500 kPa, GHSV-30,000 hr <sup>-1</sup> , and Reaction Mixture Containing 64% CH <sub>4</sub> , 16% Ar, 14% H <sub>2</sub> , 4% CO, and 2% CO <sub>2</sub> . . . . .	49
14. Conversion of CO (overall) vs. Temperature for High Loading Catalysts at 2500 kPa, GHSV-30,000 hr <sup>-1</sup> , and Reaction Mixture Containing 64% CH <sub>4</sub> , 16% Ar, 14% H <sub>2</sub> , 4% CO, and 2% CO <sub>2</sub> . . . . .	50
15. Conversion of CO (overall) vs. Temperature for High Loading Catalysts at 2500 kPa, GHSV-30,000 hr <sup>-1</sup> , and Reaction Mixture Containing 64% CH <sub>4</sub> , 16% Ar, 14% H <sub>2</sub> , 4% CO, and 2% CO <sub>2</sub> . . . . .	51
16. Conversion of CO to CH <sub>4</sub> vs. Temperature for High Loading Catalysts at 2500 kPa, GHSV-30,000 hr <sup>-1</sup> , and Reaction Mixture Containing 64% CH <sub>4</sub> , 16% Ar, 14% H <sub>2</sub> , 4% CO, and 2% CO <sub>2</sub> . . . . .	52
17. Conversion of CO (overall) vs. Temperature for High Loading Catalysts at 2500 kPa, GHSV-30,000 hr <sup>-1</sup> , and Reaction Mixture Containing 64% CH <sub>4</sub> , 12% Ar, 14% H <sub>2</sub> , 4% CO, 2% CO <sub>2</sub> , and 4% H <sub>2</sub> O . . . . .	54

LIST OF FIGURES

<u>Figure</u>		<u>Page</u>
1	Viscometer Apparatus	4
2	Temperature Dependence of Viscosity for Stripped SRC Conoco Settler Underflow (Residue 2)	5
3	Viscosity Curve for Stripped SRC Antisolvent Deashing Underflow (Residue 3)	6
4	Bench Scale Screening Unit	8
5	Effect of Coking Temperatures on Bench Screening Yields for Stripped Antisolvent Deashing Underflow (Residue 3)	9
6	Schematic Diagram of CSCU	11
7	Stirred Coker Parameter Scoping Study Stripped SRC Antisolvent Deashing Underflow	14
8	Effect of Coking Parameters on 1000°F <sup>-</sup> Product Liquid	18
9	Baytown Small Fluid Bed Coker Schematic Diagram	22

## ABSTRACT

The activity, selectivity and stability of alumina-supported nickel and nickel bimetallics in methanation of CO has been investigated during the past year. Support geometry, in situ H<sub>2</sub>S poisoning tests, and carbon deposition tests initiated during the previous contract have continued. Support geometry studies show that at high conversions and high through-put conditions monolithic supported catalysts are more active than pellet supported catalysts. In situ H<sub>2</sub>S poisoning studies show that the Ni-MoO<sub>3</sub> is more active and sulfur resistant than Ni and that H<sub>2</sub>S does not completely deactivate the surface under reaction conditions. In carbon deposition tests Ni-Pt and Ni-Co maintain catalytic activity longer than Ni. In H<sub>2</sub>S poisoning studies a synergistic effect is noted for Ni-Co compared to Ni and Co catalysts. The Ni-Co catalyst retains more activity than either Ni or Co after H<sub>2</sub>S/H<sub>2</sub> poisoning. Recent CO chemisorption experiments at various temperatures show that nickel carbonyl formation is significant at room temperature, and that CO uptakes depend greatly on the chemisorption temperature. Upper operating temperature limit tests showed that catalysts prepared in this laboratory are more active than commercial catalysts and that carbon deposition is not the only factor causing deactivation at high temperatures. These and other significant results are presented and discussed. An account of technical communications with other workers and visits to other laboratories is also included.

## I. OBJECTIVES AND SCOPE

### A. Background

Natural gas is a highly desirable fuel because of its high heating value and nonpolluting combustion products. In view of the expanding demand for and depletion of domestic supplies of clean fuels, economic production of synthetic natural gas (SNG) from coal ranks high on the list of national priorities.

Presently there are several gasification processes under development directed toward the production of SNG. Although catalytic methanation of coal synthesis gas is an important cost item in each process, basic technological and design principles for this step are not well advanced. Extensive research and development are needed before the process can realize economical, reliable operation. Specifically, there appear to be important economical advantages in the development of more efficient, stable catalysts.

From the literature (1,2), three major catalyst problems are apparent which relate to stability: (i) sulfur poisoning, (ii) carbon deposition with associated plugging, and (iii) sintering. Our understanding of these problems is at best sorely inadequate, and the need to develop new and better catalyst technology is obvious. Nevertheless, there has been very little research dealing with new catalyst concepts such as bimetallic (alloy) or monolithic-supported catalysts for methanation. This study deals specifically with sulfur poisoning, carbon deposition, and the effects of support (monolith and pellet) geometry on the performance of alloy methanation catalysts.

### B. Objectives

The general objectives of this research program are (i) to study the kinetics of methanation for a few selected catalysts tested during the first two years, (ii) to investigate these catalysts for resistance to deactivation due to sulfur poisoning and thermal degradation. The work is divided into five tasks.

Task 1. Characterize the surface, bulk and phase compositions, surface areas, and metal crystallite sizes for alumina-supported Ni, Ni-Co, Ni-MoO<sub>3</sub>, Ni-Pt, Ni-Ru and Ru catalysts.

Task 2. Continue activity testing and support geometry studies of Ni and Ni-bimetallic catalysts initiated during the first two years. The tests include (i) conversion vs. temperature runs at low and high pressures, (ii) steady-state carbon deposition tests, (iii) in situ H<sub>2</sub>S tolerance tests, and (iv) support geometry comparisons.

Task 3. Perform kinetic studies to find intrinsic rate data for alumina-supported Ni, Ni-Co, Ni-MoO<sub>3</sub>, Ni-Pt, Ni-Ru, and Ru catalysts over a range of pressures and feed compositions. Detailed rate expressions for each catalyst will be determined at low and high pressure. Effect-

iveness factors for monolithic and pellet-supported nickel on alumina will be obtained by comparing specific rates to those of finely powdered nickel on alumina.

Task 4. Determine H<sub>2</sub>S poisoning rates, thermal deactivation rates, and operating temperature limits for Ni, Ni-Co, Ni-MoO<sub>3</sub>, Ni-Pt, Ni-Ru, and Ru catalysts.

Task 5. Continue laboratory visits and technical communications. Interact closely with industrial and governmental representatives to promote large scale testing and development of the two or three best monolithic or pelleted alloy catalysts from this study.

### C. Technical Approach

The technical approach which will be used to accomplish the tasks outlined above is presented in the statement of work dated May 20, 1977. The main features of that approach are reviewed here along with more specific details and modifications which have evolved as a result of progress. It is expected that various other aspects of this approach will be modified and improved as the project develops and as new data are made available. Nevertheless, the objectives, tasks and principle features of the approach will remain the substantially the same.

#### Task 1: Catalyst Characterization

A comprehensive examination of alumina-supported Ni, Ni-Co, Ni-MoO<sub>3</sub>, Ni-Pt, Ni-Ru, and Ru catalysts will be carried out to determine surface, bulk, and phase compositions, surface areas, and metal crystallite sizes using the following techniques: chemisorption, x-ray diffraction, chemical analysis, ESCA and SIMS spectroscopy, Auger spectroscopy and transmission electron microscopy.

Hydrogen chemisorption uptakes will be measured using a conventional volumetric apparatus before each reactor test and before and after deactivation tests. X-ray diffraction measurements will be carried out to determine the active metallic phases and metal crystallite size where possible. Selected "aged" samples from Task 4 will be analyzed (by x-ray, chemical analysis, and perhaps ESCA) to determine carbon content and possible changes in phase composition or particle size. Also, transmission electron micrographs will be made to determine particle size distributions for catalyst samples. A few samples will be analyzed by EDAX to determine composition.

#### Task 2: Activity Testing and Support Geometry Design

Methanation activity and sulfur tolerance measurements initiated during the previous two years of study (3) will be completed. Pellet and monolithic alumina-supported Ni, Ni-Co, Ni-MoO<sub>3</sub>, Ni-Pt, Ni-Ru, and Ru catalysts, (both high and low metal loadings) will be activity

tested over a range of temperatures, pressures, and  $H_2S$  concentrations. A comparison of steady state conversions for nickel on different pellet and monolith supports of varying geometry will be made. Low pressure activity and sulfur tolerance tests will also be made for pelleted  $Co/Al_2O_3$  and unsupported Ni-Co and Ni-Mo alloys. A summary of the five test procedures and corresponding experimental conditions is listed in Table 1.

### Task 3: Kinetic Studies

In order to make more extensive kinetic studies of the six catalyst metal combinations a new mixed flow reactor system will be constructed. This system will be capable of operation to 7500 kPa and 775 K and over a range of reactant compositions. The reactor for this system will be a "Berty" type constant volume mixed flow Autoclave reactor.

Intrinsic rate data will be obtained for alumina-supported Ni, Ni-Co, Ni-MoO<sub>3</sub>, Ni-Pt, Ni-Ru, and Ru catalysts over a range of pressures and feed compositions in order to obtain detailed rate expressions at low and high pressures. To insure gradientless operation in the reaction-limited regime the rates will be measured at low conversions (0-5%) and low temperatures (525-600 K) for samples which have been crushed to obtain small particles.

Isothermal effectiveness factors for monolithic and pellet-supported nickel on alumina will be obtained by comparing their specific rates to those of finely powdered nickel on alumina using the same mixed flow reactor.

### Task 4: Degradation Studies

$H_2S$  poisoning rates and thermal deactivation rates at low pressure will be studied using a new quartz reactor system. Quartz was selected as the material for the reactor because it must operate at high temperatures (750-1000 K) and in a corrosive ( $H_2S$ ) environment. This reactor is also a constant volume mixed flow type reactor according to the design of Katzer (4). The quartz reactor system will be constructed during the early part of the contract period. Thermal deactivation at high pressures will be studied using a tubular stainless steel reactor previously discussed (3).

Operating temperature limits (and specific reaction rates within this range), thermal deactivation rates near the upper use temperature (in the presence and absence of steam), and  $H_2S$  poisoning rates (at 525 K in the presence of 1 and 10 ppm  $H_2S$  in  $H_2$ ) will be determined for Ni, Ni-Co, Ni-MoO<sub>3</sub>, Ni-Pt, Ni-Ru, and Ru catalysts. The extent of carbon-carbide deposited in the thermal deactivation runs will be determined by chemical analysis and x-ray diffraction.

Table 1

## Description of Reactor Tests for Task 2

<u>Test Procedures</u>	<u>Experimental Conditions</u>
1. <u>Temperature-Conversion Test</u> : Measure CO conversion and methane production as a function of temperature, with and without 1% (by vol.) of steam present in the reactant mixture.	475-675 K 140 kPa 30,000 hr <sup>-1</sup> 1% CO, 4% H <sub>2</sub> , 95% N <sub>2</sub> (dry basis)
2. <u>Temperature-Conversion Test (high pressure)</u> : Measure CO conversion and methane production as a function of temperature at 2500 kPa.	475-675 K 2500 kPa 30,000 hr <sup>-1</sup> 1% CO, 4% H <sub>2</sub> , 95% N <sub>2</sub>
3. <u>Steady State (24 Hr.) Carbon Deposition Test</u> : Measure CO conversion and methane production at 500 and 525 K (250,000 hr <sup>-1</sup> ) before and after an exposure of 24 hours at 675 K.	675 K (24 hrs.) 140 kPa 200,000-250,000 hr <sup>-1</sup> 25% CO, 50% H <sub>2</sub> , 25% N <sub>2</sub> H <sub>2</sub> /CO = 2
4. <u>In situ H<sub>2</sub>S Tolerance Test</u> : Measure intermittently the production of methane and hydrocarbons (by FID) during 24 hours exposure to feed containing 1 or 10 ppm H <sub>2</sub> S using a glass reactor.	525 K 140 kPa 30,000 hr <sup>-1</sup> 1% CO, 4% H <sub>2</sub> , 95% N <sub>2</sub> 1 or 10 ppm H <sub>2</sub> S
5. <u>Support Geometry Tests</u> : Measure CO conversion and methane production as a function of temperature for the same Ni/Al <sub>2</sub> O <sub>3</sub> catalyst supported on monoliths and pellets of varying geometries.	575-675 K 140 kPa 30,000 hr <sup>-1</sup> 1% CO, 4% H <sub>2</sub> , 95% N <sub>2</sub>

### Task 5: Technical Interaction and Technology Transfer

The principal investigator will continue to communicate closely with other workers in methanation catalysis, continue distribution of quarterly reports to selected laboratories to stimulate interest and feedback, attend important coal and catalysis meetings, and visit other methanation laboratories.

He will also interact closely with Mr. A.L. Lee at the Institute of Gas Technology, with personnel at the Pittsburgh Energy Research Center and with other coal gasification representatives to promote large scale testing and development of the two or three best catalysts from this study.

## II. SUMMARY OF PROGRESS

A project progress summary is presented in Figure 1 and accomplishments during the past year are summarized below. Figure 1 shows that task accomplishments are either on or ahead of schedule.

Accomplishments and results from the past year are best summarized according to task:

Task 1. Over the past year several new catalysts were prepared, including 9 pelleted, 20 cordierite monolithic, 9 alumina monolithic, and 16 Torvex monolithic catalysts with active metal combinations of Ni, Ni-Co, Ni-MoO<sub>3</sub>, Ni-Pt, and Ni-Ru. Catalysts prepared during the previous contract period (3) were also further characterized as part of this task. Hydrogen chemisorption uptake, an indication of active metal surface area, was measured before and after reactor tests for all catalysts. Many catalysts were further characterized by chemical analysis, x-ray diffraction, electron microscopy, Auger electron spectroscopy and ESCA. Some tests of the reliability of CO chemisorption on nickel catalysts near room temperature have also been performed.

While hydrogen chemisorption at room temperature is a reliable means of measuring active metal surface area (3), CO chemisorption at room temperature causes nickel carbonyl formation. Data obtained during the last quarter reveal that the amount of nickel carbonyl formed and CO adsorbed varies with the temperature history of the sample. However, hydrogen chemisorption uptakes before and after CO chemisorptive measurements do not vary significantly.

Transmission electron micrographs of catalysts samples and the blank alumina support have shown that increased contrast between the support and the metal phase is necessary for more definitive work. Our electron microscope technician is using a new Phillips microscope in order to improve this characterization technique.

Task 2. Much of the activity testing was completed during the first quarter. However, selected experiments in the areas of sulfur poisoning and carbon deposition are still in progress to answer important questions which have arisen during the execution of this task.

During the first quarter, steady state carbon deposition tests were performed on 5 monolithic catalysts. The order of activity after 24 hours testing in a H<sub>2</sub>/CO = 2 mixture (5% CO) at 400°C was Ni-Pt > Ni-Co > Ni-Ru > Ni > Ni-MoO<sub>3</sub>.

In situ H<sub>2</sub>S tolerance tests were performed on powdered catalysts in a reaction mixture containing 10 ppm H<sub>2</sub>S. After 24 hours, the order of activity for 3-6 wt.% catalysts was Ni-MoO<sub>3</sub> > Ni = Ni-Rh > Ni-Ru. Similar tests on high loading samples (14-20%) gave the following order: Ni > Ni-Co > Ni-Pt. The order of activity for monolithic catalysts was Ni-MoO<sub>3</sub> > Ni > Ni-Co > Ni-Ru > Ni-Pt. Tests of the gases downstream of 3% Ni-Rh catalyst showed gradual H<sub>2</sub>S breakthrough

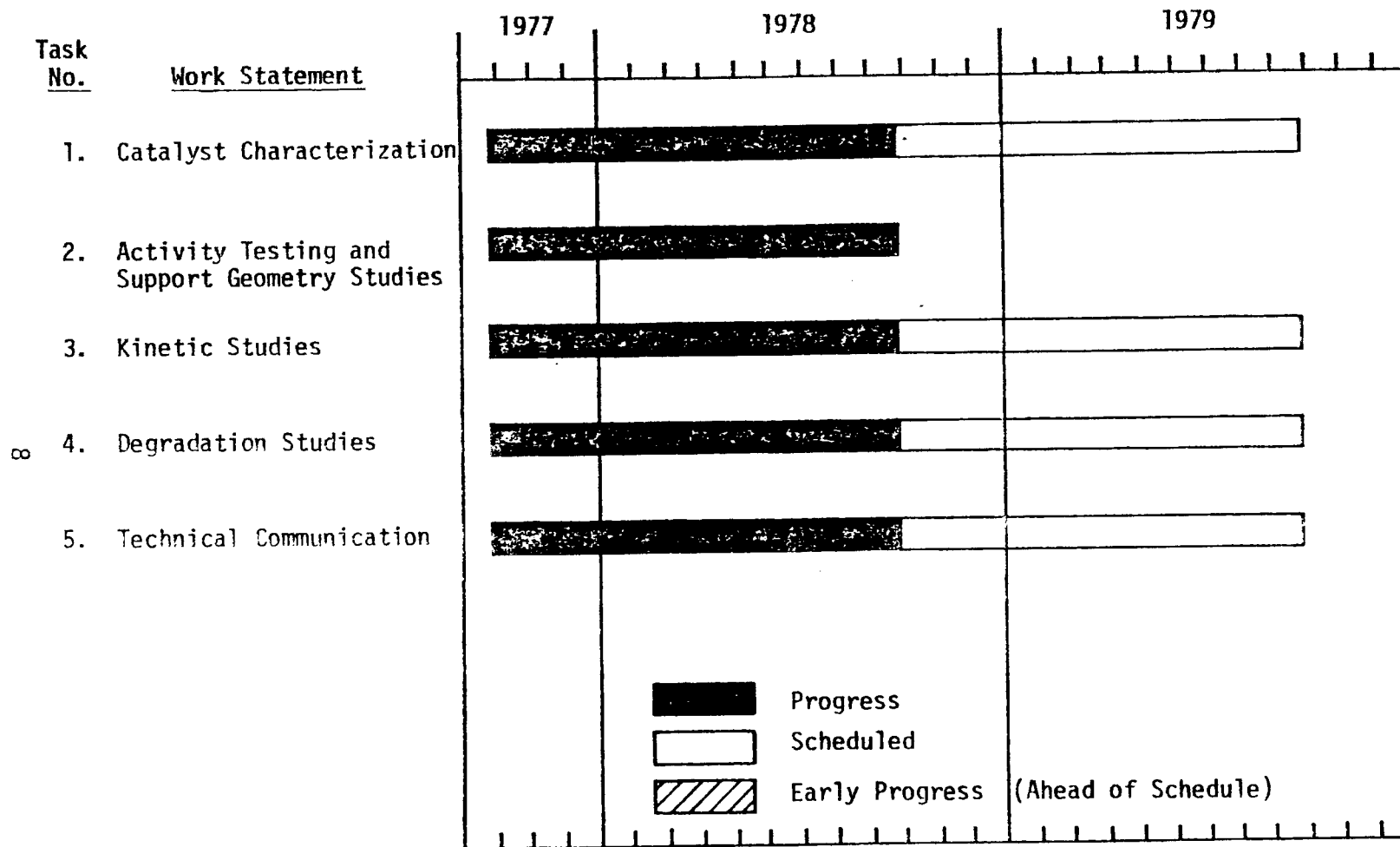


Figure 1. Project Progress Summary.

much earlier than expected. Apparently, equilibrium  $H_2S$  adsorption does not occur under reaction conditions, possibly because of competitive adsorption of reacting species.

Activity measurements of pelleted and powdered Ni-Co-A-100 showed that the powdered sample loses much more specific activity after treatment in 10 ppm  $H_2S/H_2$  than the pelleted sample. Thus, catalyst geometry plays an important role in the poisoning process. A pore mouth or shell type poisoning model is consistent with these data. Also, activity tests on powdered Ni, Ni-Co, and Co catalysts before and after  $H_2S$  poisoning in a fluidized bed show a synergistic effect for Ni-Co. The poisoned site activity ratio (PSAR) is much higher (about a factor of 2) than either the Ni or Co catalysts.

Support geometry studies were performed on nickel catalysts to compare pellets with various monolith configurations. In these tests at high through-put conditions, monolithic catalysts were significantly more active for methanation than the catalyst pellets. The substantially lower pressure drop through the monolithic catalyst would enable it to be operated at much higher space velocities. Accordingly, a reactor containing monolithic catalysts would be significantly smaller than a corresponding pellet reactor, resulting in a substantial savings in capital investment. The low pressure drop could be translated into a savings in operating cost.

Task 3. The Berty reactor system for high pressure kinetic studies was constructed during the first year. Preliminary tests showed that it is operational. Also, a Haskell gas compressor was installed for making high pressure gas mixtures.

Task 4. Upper operating temperature limit tests, both with and without reactant steam, have been performed on five catalyst combinations and two commercial catalysts. Methane was the major diluent gas in the reactant mixture. Tests without steam showed that catalysts prepared in this laboratory are more active than commercial catalysts at high temperatures and pressures. High temperature tests with reactant steam (4%) showed that all the catalysts lose activity similar to the tests without steam. This suggests that carbon deposition is not the only factor in the loss of activity since steam would tend to prevent carbon formation. Also, with reactant steam, negative CO to  $CH_4$  conversions were found above 775 K. The diluent  $CH_4$  appears to be reformed to CO and  $CO_2$  under these reaction conditions.

Task 5. During the first year, the principal investigator attended the Fall Meeting of the California Catalysis Society and presented a paper. Along with eight students, he attended the Third Rocky Mountain Fuel Symposium and was instrumental in organizing the Rocky Mountain Fuel Society. Also, he attended a conference on Catalyst Deactivation and Poisoning at the Lawrence Berkeley Laboratory and the 85th National Meeting of the AIChE in Philadelphia and presented a paper at each of these meetings. He participated in a workshop sponsored by NSF at the University of Maryland where the future basic research needs and goals in catalysis research were assessed. The Principal Investigator visited catalysis research laboratories at

the University of Kentucky - Institute for Mining and Minerals Research, Los Alamos Scientific Laboratory, Norton Chemical Company in Akron, Ohio, Climax Molybdenum Company of Michigan and Gulf Research Company in Pittsburgh and presented seminars at each laboratory.

Five graduate and three undergraduate students have contributed to this research project. Two students have written master's theses and three students have Ph.D. research underway.

### III. DETAILED DESCRIPTION OF TECHNICAL PROGRESS

#### Task 1: Catalyst Characterization

##### 1. Catalyst Preparation

During the first year, eight pellet catalysts and several monolith catalysts were prepared. Compositions of the pellet catalysts are listed in Table 2; they were prepared using impregnation techniques similar to those previously reported (3). However, since these catalysts were to be tested at high temperatures, the Kaiser SAS 5x8 mesh alumina pellets were calcined 3 hours at 1075 K before impregnating with aqueous solutions of the nitrate salts.

Since chloride ions act to poison the methanation reaction, Ni-Ru and Ni-Pt pellet catalysts were prepared from chloride-free salts. The Ni-Ru catalyst preparation and the preparation of the impregnating solution for Ni-Pt were described earlier (7). However, the Ni-Pt catalyst was calcined in air for three days at 423 K and one day at 473 K. During reduction, a very slow temperature ramp was used where the catalyst remained below 473 K for ten hours. The temperature was then slowly raised to 673 K and held there for ten hours.

Several monolithic Ni catalysts were prepared for the support geometry studies in Task 2. Pure alumina monoliths were obtained from Corning Glass Works and prepared similarly to cordierite monoliths (5). Several Torvex Ceramic Honeycombs (DuPont Co.) were also prepared. Some of these had an activated alumina wash coat applied by the manufacturer. Our lab applied an alumina wash coat to the rest (7). Instabilities of the wash coats at high metal loadings were noted in QPR-2 (6). Several monolith Ni catalysts supported on  $Al_2O_3$  cordierite were also prepared. Data summarizing the preparation of monolithic catalysts are listed in Table 2 with notes about the support geometries, wash coats, etc.

##### 2. Chemisorption

During the first year, hydrogen chemisorption measurements were performed on ten pellet catalyst samples before and after reactor testing and on five alumina monolith, two powder catalyst and three cordierite monolith samples before reactor testing. The results are listed in Table 3.

Catalyst samples used in upper operating temperature tests generally had lower uptakes than fresh samples (see Table 3). Apparently, sintering occurred after runs with steam. Some of the monolith and pellet samples disintegrated because of massive carbon deposition. Hydrogen chemisorption uptakes for these samples increased. This may be explained by surface restructuring and crystallite fracture during the carbon deposition process.

Table 2  
Catalyst Codes and Compositions

<u>Catalyst</u>	<u>Code</u>	<u>Composition</u>	<u>Comments</u>
Ni/Al <sub>2</sub> O <sub>3</sub>	Ni-A-120	3% Ni	Pellets
Ni/Al <sub>2</sub> O <sub>3</sub>	Ni-A-121	6% Ni	Pellets
Ni/Al <sub>2</sub> O <sub>3</sub>	Ni-A-122	20% Ni	Pellets
Ni-Co/Al <sub>2</sub> O <sub>3</sub>	Ni-Co-A-102	3% Ni, 3% Co	Pellets
Ni-Co/Al <sub>2</sub> O <sub>3</sub>	Ni-Co-A-103	10% Ni, 10% Co	Pellets
Ni-MoO <sub>3</sub> /Al <sub>2</sub> O <sub>3</sub>	Ni-MoO <sub>3</sub> -A-105	10% Ni, 10% MoO <sub>3</sub>	Pellets
Ni-Ru/Al <sub>2</sub> O <sub>3</sub>	Ni-Ru-A-108	2.5% Ni, 0.5% Ru	Pellets, Chloride free
Ni-Pt/Al <sub>2</sub> O <sub>3</sub>	Ni-Pt-A-101	15.7% Ni, 0.5% Pt	Pellets, Chloride free
Ni-Pt/Al <sub>2</sub> O <sub>3</sub>	Ni-Pt-A-102	2.5% Ni, 0.5% Pt	Pellets, Chloride free
Ni/NiAl <sub>2</sub> O <sub>4</sub>	Ni-NAL-100	15% Ni	Extrudates, nickel alumi- nate support
Ni/Al <sub>2</sub> O <sub>3</sub>	Ni-M-160 to 167	~20% Ni	Cordierite monolith with alumina wash coat
Ni/Al <sub>2</sub> O <sub>3</sub>	Ni-M-169 to 174	~22% Ni	Cordierite monolith with alumina wash coat
Ni/Al <sub>2</sub> O <sub>3</sub>	Ni-M-175 to 181	~17% Ni	Cordierite monolith with alumina wash coat
Ni/Al <sub>2</sub> O <sub>3</sub>	Ni-AM-101 to 105	~29% Ni	Alumina monoliths 31 squares/cm <sup>2</sup>
Ni/Al <sub>2</sub> O <sub>3</sub>	Ni-AM-201 to 204	~26% Ni	Alumina monoliths 36 triangles/cm <sup>2</sup>
Ni/Al <sub>2</sub> O <sub>3</sub>	Ni-TM-110 to 357	~3% Ni	Torvex monoliths with alumina wash coat

Table 3

Summary of Metal Surface Area  
Measurements Using H<sub>2</sub> Chemisorption  
at 25°C

<u>Catalyst</u>	<u>Nominal Composition (wt.%)</u>	<u>Uptake (<math>\mu</math>moles/gram)</u>	<u>Maximum Reactor (1) Temperature</u>
<u>Pellet Catalysts:</u>			
Ni-A-120	3% Ni	31.0 <sup>a</sup>	
Ni-A-121	6% Ni	73.9 <sup>a</sup>	
Ni-A-122	20% Ni	212.7 <sup>a</sup>	763 K
		209.8 <sup>b,h</sup>	
		175.5 <sup>b</sup>	
		172.8 <sup>b</sup>	
		157.0 <sup>c</sup>	835
Ni-Co-A-102	3% Ni, 3% Co	37.6 <sup>a</sup>	
Ni-Co-A-103	10% Ni, 10% Co	117.4 <sup>a</sup>	725
		94.0 <sup>b</sup>	
		78.8 <sup>c</sup>	
			825
Ni-MoO <sub>3</sub> -A-105	10% Ni, 10% MoO <sub>3</sub>	52.8 <sup>a</sup>	816
		46.6 <sup>b</sup>	
		58.2 <sup>c</sup>	
			820
Ni-Pt-A-101	15.7% Ni, 0.5 Pt	211.4 <sup>a</sup>	820
		138.4 <sup>b</sup>	
		123.7 <sup>c</sup>	
			825
Ni-NAL-100	15% Ni	29.0 <sup>a</sup>	803
		209.4 <sup>a,f</sup>	
		162.3 <sup>b</sup>	
		184.5 <sup>c</sup>	
			818
G-87P		138 <sup>a</sup>	800
		118.6 <sup>b</sup>	
		162.8 <sup>c</sup>	
			822
MC-100		130.7 <sup>a</sup>	820
		178.7 <sup>b,h</sup>	
		81.9 <sup>c</sup>	
			793
Ni-Co-A-100	10% Ni, 10% Co	107 <sup>a</sup>	
		0 <sup>d</sup>	
		4 <sup>e</sup>	
		80 <sup>a,f</sup>	
		134 <sup>a,g</sup>	

<u>Catalyst</u>	<u>Nominal Composition (wt.%)</u>	<u>Uptake (<math>\mu</math>moles/gram)</u>	<u>Maximum Reactor (1) Temperature</u>
Ni-Rh-A-100	2.5% Ni 0.5% Rh	19.0 <sup>a</sup> 0 <sup>d</sup>	
Ni-Pd-A-100	15% Ni 1% Pd	105 <sup>a,g</sup> 99 <sup>a,g</sup> 112 <sup>a,g</sup>	
<u>Monolith Catalysts:</u>			
Ni-AM-101	29.7% Ni	221.7 <sup>a</sup>	
Ni-AM-102	27.8% Ni	196.0 <sup>a</sup>	
Ni-AM-201	25.5% Ni	201.1 <sup>a</sup>	
Ni-AM-203	25.5% Ni	179 <sup>a</sup>	
Ni-AM-204	27.5% Ni	204.5 <sup>a</sup>	
Ni-M-250	22.2% Ni	154.8 <sup>a</sup>	
Ni-M-179	17% Ni	87.3 <sup>a</sup>	
Ni-M-180	17% Ni	138.0 <sup>a</sup> 84.0 <sup>c</sup>	818

Powders

Ni-Co-A-100 before poisoning	10% Ni, 10% Co	148.2 <sup>i</sup>
Ni-Co-A-100 after poisoning		67.7 <sup>i</sup>

(1) This column shows the maximum temperature in degrees Kelvin achieved during upper operating temperature limit tests.

<sup>a</sup>Bulk reduced

<sup>b</sup>Upper operating temperature limit tested without steam

<sup>c</sup>Upper operating temperature limit tested with steam

<sup>d</sup>Long term H<sub>2</sub>S in situ poisoning tested

<sup>e</sup>Long term H<sub>2</sub>S in situ poisoning tested followed by CO and air regeneration

<sup>f</sup>Reduced an additional 2 to 4 hours

<sup>g</sup>Reduced an additional 10 to 15 hours

<sup>h</sup>Catalyst support disintegrated after reactor test

<sup>i</sup>Differentially reactor tested

Some of the catalyst samples were chemically analyzed for carbon content by Rocky Mountain Geochemical, Salt Lake City. The data from these tests is shown in Table 4. After Runs B and C, samples of Ni-A-122 contained large amounts of carbon. Both of these samples were observed to deactivate rapidly before the test was ended. A sample which had not been reactor run contained very little carbon (0.15%); Ni-Co and Ni-MoO<sub>3</sub> samples also contained very little carbon (<.5%) after testing. The small amount of carbon on these samples suggests that carbon deposition may not be the only factor in the deactivation process. All of these samples lost H<sub>2</sub> uptake during the tests at high temperature.

During the last quarter, a series of chemisorption measurements were made on a 3% nickel on alumina catalyst using hydrogen and carbon monoxide as the adsorbate gases. The purpose of the experiments was to determine if significant amounts of nickel carbonyl are formed at the temperatures tested and to develop an experimental procedure to be used for further testing of sulfided catalysts during the next quarter. Ni(CO)<sub>4</sub> was decomposed to metallic Ni in a small diameter pyrex tube maintained at 573 K (the temperature for decomposition of nickel carbonyl is 453 K) which was weighed accurately before and after the titration gas was passed through it to determine the amount of nickel deposited on the inner surface. The results of the experiments are found in Table 5. As can be readily seen, the results are not entirely consistent. The variation in the amount of CO adsorbed can be explained by variations in the pretreatment history (e.g. order of H<sub>2</sub> and CO adsorption) and by other variables such as the temperature of adsorption and the temperature at which CO was evacuated or flushed from the cell. The large values for the CO uptake reported for samples 3A and 4B are possibly the result of O<sub>2</sub> impurities in the helium passed directly over the catalyst to flush out the titration gas between isotherms and/or restructuring of the surface due to Ni(CO)<sub>4</sub> formation during the previous CO adsorption. Impurity problems were avoided in later experiments by pumping the titration gas from the cell and trapping the Ni(CO)<sub>4</sub> in a cold trap. The cold trap was separated from the cell and flushed with He. Runs on Samples 2A and 6C resulted in CO:H ratios more in line with previous results.

The amount of nickel detected from Ni(CO)<sub>4</sub> decomposition was found to vary somewhat due to some carbon deposition caused by a thermocouple inserted into the collection device. No formation of nickel carbonyl was detected for Run 2A, although there was some detected for Run 7C. In the latter case, this effect is probably due to the fact that the titration cell in 7C was allowed to warm up to room temperature, resulting in the formation of the carbonyl at the higher temperature. The data in Run 2A suggest that no Ni(CO)<sub>4</sub> is formed at 187 K. Tests begun recently in the 5th quarter confirm no formation of nickel carbonyl at this temperature.

During the next quarter, more tests will be conducted on fresh and sulfided samples of the same catalyst. The samples will be tested at 190, 273 and 298 K for the formation of nickel carbonyl and carbonyl sulfide. The procedure developed during this quarter will be further refined and presented in more detail in the next quarterly report.

Table 4

## Carbon Analysis of Catalyst Samples

<u>Catalyst</u>	<u>History</u>	<u>Carbon Content (wt.%)</u>
Ni-A-122	Bulk reduced	0.15
Ni-A-122	Upper operating temperature tested - Run A	0.40
Ni-A-122	Upper operating temperature tested - Run B	35.78
Ni-A-122	Upper operating temperature tested - Run C	30.44
Ni-Co-A-103	Upper operating temperature tested	0.42
Ni-MoO <sub>3</sub> -A-105	Upper operating temperature tested	0.30

Table 5

Comparison of Carbon Monoxide and Hydrogen  
Chemisorption Measurements on 3% Nickel  
on Alumina Powdered Catalyst

Run <sup>a</sup> #	Temp K	Adsorbate Gas	Uptake $\mu\text{moles/g}$	CO/H	Ni. from $\text{Ni}(\text{CO})_4$ decomposition (g)
1A	292	H <sub>2</sub>	29.1		
2A	187	CO	97.9	1.68	
3A	295	CO	184.6	3.17	.0063
4B	298	CO	179.6	3.08	.0016
5C	298	H <sub>2</sub>	25.7		
6C	294	CO	113.56	2.21	.0031
7C	185	CO	61.04	1.19	.0011
8C	296	H <sub>2</sub>	26.4		

<sup>a</sup>Runs with the same alphabetic suffix represent measurements of the same catalyst sample.

### 3. Transmission Electron Microscopy

Transmission electron microscopy (TEM) measurements of Ni-MoO<sub>3</sub>-A-103, Ni-A-119, Ni-Co-A-100, Ni-A-121 and the Kaiser SAS alumina support were carried out during the contract period. The average crystallite diameters determined from TEM are shown in Table 5A and compared with estimates from x-ray diffraction and H<sub>2</sub> chemisorption measurements.

During the third quarter, a slight modification to the procedure recorded in previous reports was made. A holey formvar coated grid was implemented in place of the non-hole formvar coated grid. The purpose of this grid support modification is to provide better resolution of the catalyst. When the ground catalyst is placed on the holey formvar coated grids a good percentage of the catalyst particles will appear above a hole. This method eliminates any inconsistencies that may arise due to the support, such as variable thickness of the support causing resolution problems or contamination on the support which could affect also the micrograph.

In Figures 2 and 3, the number percent of particles is given for each size range of fresh and sintered (at 1023 K) Ni-A-119 (15% Ni/Al<sub>2</sub>O<sub>3</sub>). For the fresh sample, 76% of the particles are less than 3.7 nm, but only 18% are less than 3.7 nm for the sintered sample. It appears that in the sintered sample the larger particles grew at the expense of particles in the lower size ranges. The particle distribution in the fresh sample is very steep with most particles less than 3.7 nm and none more than 6.7 nm. However, the sintered sample has a very broad particle distribution with a significant fraction of the particles less than 3.0 nm and greater than 10.0 nm. This suggests that the mechanism for sintering may be atomic migration (8) since redispersion occurs in the particle size range of <3.0 nm and because growth occurs above 5.0 nm where continued growth by metal crystallite migration might not be possible.

During the third quarter, we noted a problem with metal-support contrast in our micrographs from the Hitachi instrument. Micrographs of the blank alumina support, showed the structural appearance of some areas to be quite like that of a metal impregnated support (see Figures 4 and 5). However, many of the alumina-supported nickel showed enough contrast between the support and metal particles. Our electron microscope technician is presently learning how to use a Phillips 400 Electron Microscope with which we are confident the contrast between support and metal can be improved.

### 4. X-Ray Diffraction Scans

Samples of Ni-A-116, Ni-Co-100 and Ni-MoO<sub>3</sub>-102 were submitted to the University of Kentucky Institute of Mining and Metallurgical Research for x-ray diffraction analysis. During the fourth quarter, data were obtained for Ni-Co-100 and Ni-MoO<sub>3</sub>-102. In the case of Ni-Co-100, peaks for  $\gamma$ -Al<sub>2</sub>O<sub>3</sub> and the metallic constituents were observed; unfortunately, the metal peaks were sufficiently broad and overlapping to prevent assignment of the peaks to either Ni, Co or Ni-Co. Thus,

Table 5A

Comparison of Particle Sizes Calculated  
from X-ray Line Broadening  
Hydrogen Adsorption, and Electron Microscopy

<u>Catalyst</u>	<u>X-ray plane</u>	<u>X-ray</u>	<u>d particle (Å)</u> <u>H<sub>2</sub> Adsorption</u>	<u>Electron microscopy</u>
Ni-A-115 (25% Ni/Al <sub>2</sub> O <sub>3</sub> )	(200) (200)	53.2 36.4	65.3	68
Ni-A-114	(200)	32.3	46.4	53
Ni-Co-A-100	(200) (102) (225) or (110)	95.3 77.7 88.8	99.1	51
Ni-MoO <sub>3</sub> -A-103	--	--	89.5	41

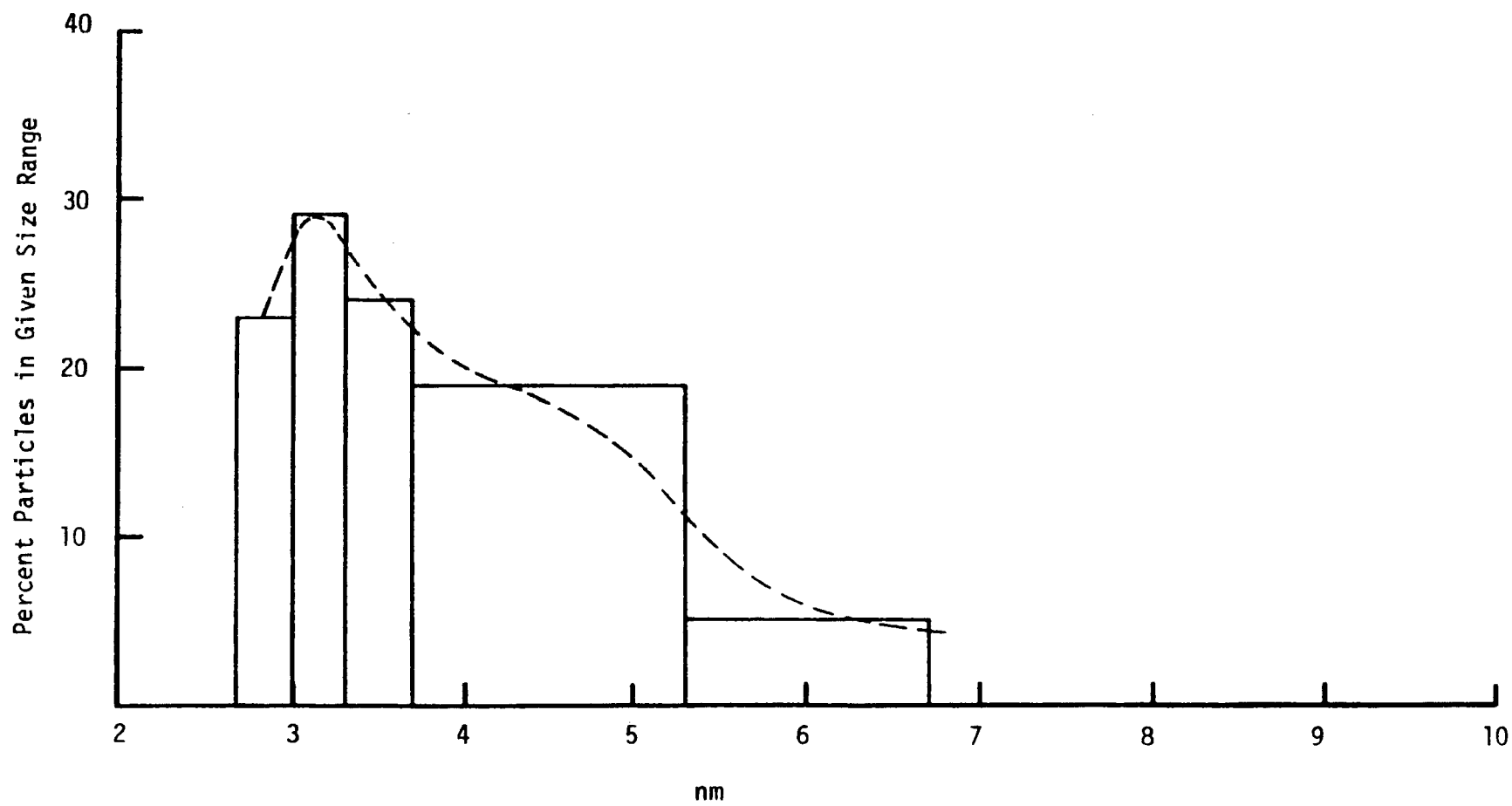


Figure 2. Particle size distribution of Ni-A-119 before sintering.

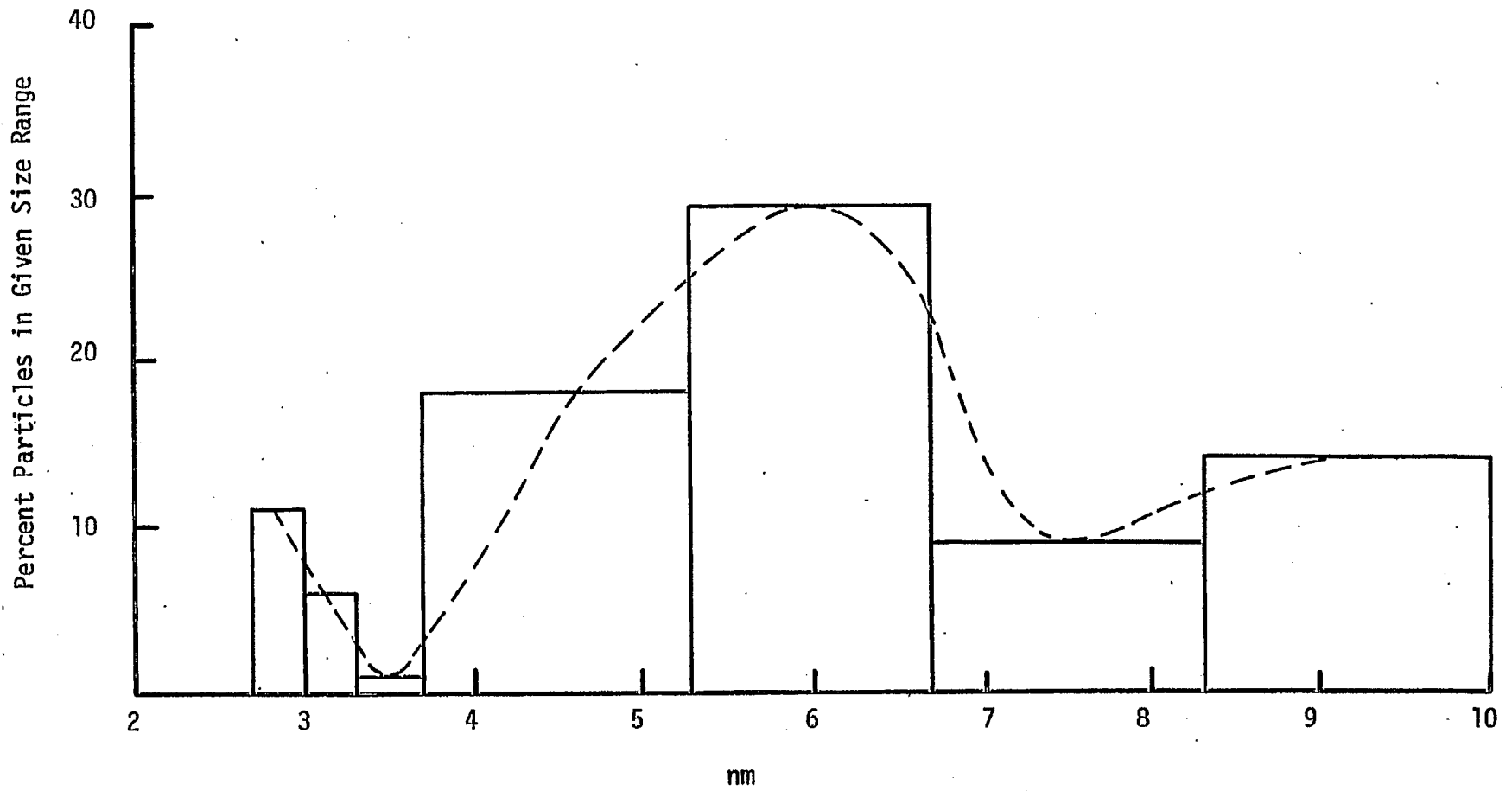


Figure 3. Particle size distribution of Ni-A-119 after sintering.



Figure 4. Electron micrograph of BL-A-101 (blank alumina support) 295,000x.

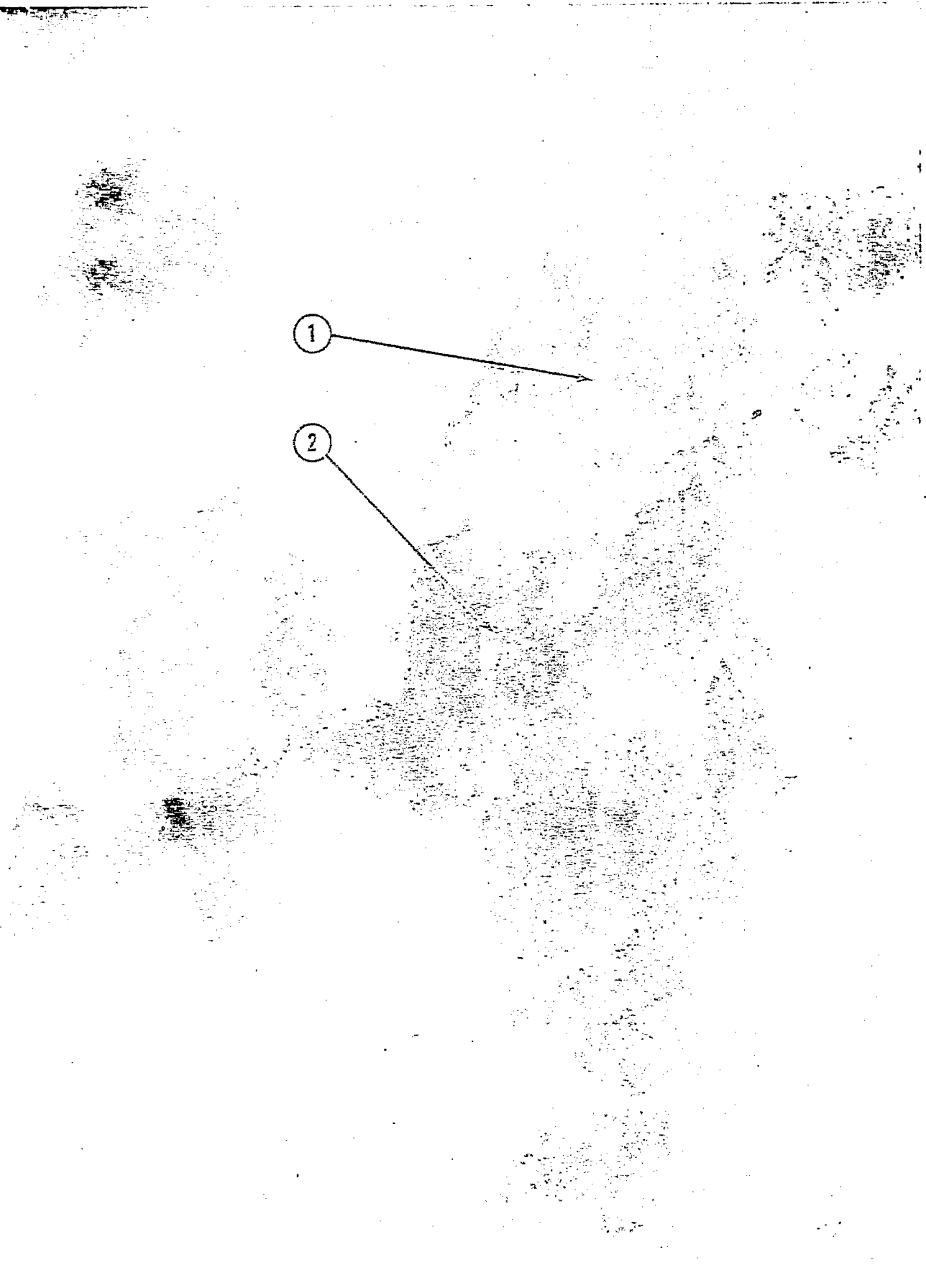


Figure 5. Electron micrograph of Ni-A-121 (6% Ni) 295,000x.

Reproduced from  
best available copy

the data do not confirm nor rule out the possibility of alloy formation. The scan for Ni-MoO<sub>3</sub>-102 revealed peaks assignable only to  $\gamma$ -Al<sub>2</sub>O<sub>3</sub>. Hence, the nickel crystallites are apparently masked by the Al<sub>2</sub>O<sub>3</sub> and/or are x-ray amorphous. This suggests that very small particles (<3.0 nm) are predominant in the sample, consistent with TEM data presented earlier for the same sample (3, 6, 7). Since H<sub>2</sub> chemisorption uptakes are lower than would be expected for such small particles, the data (see Table 5A) suggest that Ni and MoO<sub>2</sub> or MoO<sub>3</sub> may interact strongly preventing adsorption of H<sub>2</sub> on some of the nickel sites.

## Task 2: Activity and Support Geometry Tests

### 1. Steady State Carbon Deposition Tests:

The reaction conditions for the monoliths were changed from those employed for powdered catalysts (20% CO, 40% H<sub>2</sub>) because of difficulties controlling temperature in the tests of powdered samples. Accordingly, each of the monolithic catalysts samples listed in Table 6 was exposed to a gas mixture containing 5% CO and 10% H<sub>2</sub> for an extended period of time at 673 K and then tested for methanation activity. Activity, the ratio of fouled rate to fresh rate, is plotted in Figure 6 as a function of time. Activity was measured before and after exposure and at one intermediate time by lowering the temperature to 523 K and adjusting the flow to obtain the standard reaction mixture for activity testing.

The data in Figure 6 and Table 6 show that, except for Ni-Pt, all of the catalysts lost more than 25% of their initial activity within the first 12 hours. Based on these data, the order of decreasing resistance to carbon deposition is Ni-Pt > Ni-Co > Ni-Ru > Ni > Ni-MoO<sub>3</sub>. These results are in qualitative agreement with results of carbon deposition tests reported earlier for pellet-supported catalysts having about the same nominal compositions (3). Apparently, Ru, Co and Pt act in combination with nickel as promoters to slow the rate of carbon deposition. Pt is the most effective, especially in view of its very low concentration in the Ni-Pt catalyst of only 0.6 wt.% (2% with respect to the metal).

An attempt to regenerate the deactivated nickel-molybdate monolith was made using hydrogen at 573 K for six hours. The turnover number for methanation following this treatment was  $4.9 \times 10^{-3}$  molecules/site/second. This value is a factor of 3 larger than the value of 1.75 reported after 24 hours, but, unfortunately, is still a factor of 10 lower than the initial activity. While oxygen treatments are generally used to burn off carbon deposits, it is interesting that hydrogen alone can restore 10% of the initial activity. Apparently, 10% of the carbonaceous deposit is active carbon which can be removed by hydrogenation while the remaining 90% is inactive.

### 2. In situ H<sub>2</sub>S Tolerance Tests:

a. Powdered Samples. H<sub>2</sub>S in situ poisoning tests were conducted on seven Ni and Ni bimetallic catalysts. Early tests were conducted

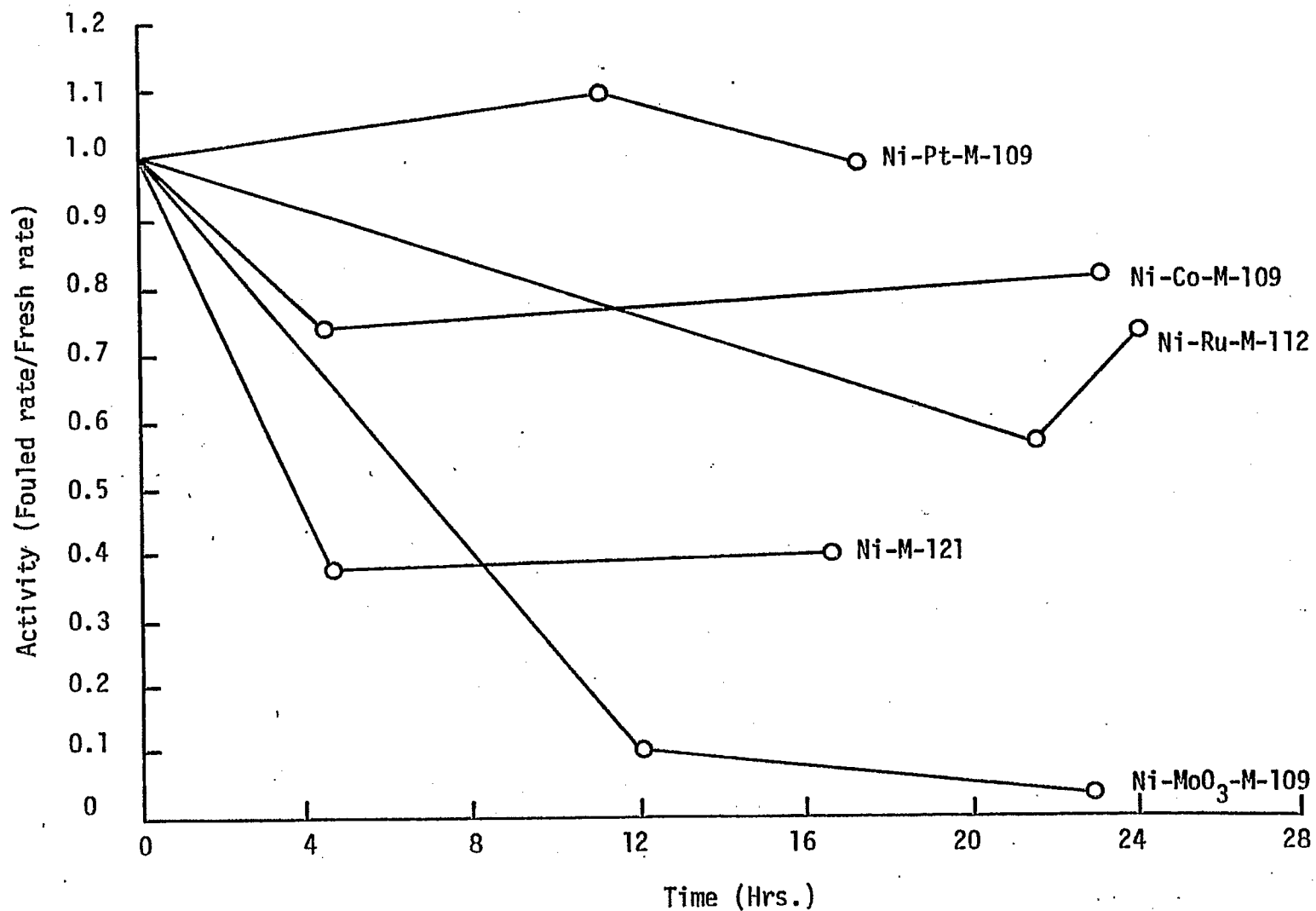


Figure 6. Activity versus Time during Carbon Deposition Tests for Various Monolithic Catalysts (Test Conditions: 673 K, 75,000 hr<sup>-1</sup> GHSV, 100 kPa, 85% N<sub>2</sub>, 10% H<sub>2</sub>, 5% CO. Activity measured at: 523 K, 80,000 hr<sup>-1</sup> GHSV, 100 kPa, 95% N<sub>2</sub>, 4% H<sub>2</sub>, 1% CO, 1 atm).

Table 6

Results of Carbon Deposition Tests of Monolithic-Supported Nickel and Nickel Bimetallic Catalysts  
 (Deposition occurred at 673K, 75,000 hr<sup>-1</sup> GHSV, 85% N<sub>2</sub>, 10% H<sub>2</sub>, 5% CO.  
 Activity was measured at 523K, 80,000 hr<sup>-1</sup> GHSV, 95% N<sub>2</sub>, 4% H<sub>2</sub>, & 1% CO)

Catalyst	Composition	Methane <sup>a</sup> Turnover Number, Fresh Catalyst	Time (hr.)	Turnover Number Fouled Catalyst	Fouled Activity <sup>b</sup>
Ni-M-121	6% Ni, 20% alumina 74% ceramic	36.6	4.5	13.7	.37
			16.5	14.7	.40
Ni-Co-M-106	4.8% Nickel 4.8% Cobalt 19.6% alumina 70.8% ceramic	17.8	4.25	13.3	.75
			23.0	14.6	.82
Ni-MoO <sub>3</sub> -M-101	4% Nickel 4% Molybdate 20% alumina 72% ceramic	43.5	12.0	4.6	.11
			22.8	1.75	.04
Ni-Pt-M-109	10.3% Nickel .55% Platinum 19.7% alumina 69.5% ceramic	11.1	11.0	12.2	1.10
			17.0	11.0	.99
Ni-Ru-M-112	10% Nickel 1% Ruthenium 18.5% alumina 70.5% ceramic	2.37	21.5	1.36	.57
			24.0	1.75	.74

<sup>a</sup>Turnover numbers are expressed as molecules of methane formed per active site per second.

<sup>b</sup>Activity is defined here as the ratio of the specific rate after testing to the initial specific rate.

at 523 K with a GHSV of  $30,000 \text{ hr}^{-1}$  and a reactant gas mixture of 95%  $\text{N}_2$ , 4%  $\text{H}_2$ , 1%  $\text{CO}$  and 10 ppm  $\text{H}_2\text{S}$ , using  $0.1 \text{ cm}^3$  powdered catalyst samples. Later tests were performed with 99%  $\text{H}_2$ , 1%  $\text{CO}$  and 10 ppm  $\text{H}_2\text{S}$  as reactants, as noted below.

The activity (poisoned rate/fresh rate) versus time is plotted in smooth curves in Figure 7 for each of the catalysts. A brief summary of the data is listed in Table 7. For the high loading catalysts, the order of decreasing sulfur tolerance is apparently  $\text{Ni} > \text{Ni-Co} > \text{Ni-Pt}$ . For the 3-5 wt.% catalysts:  $\text{Ni-MoO}_3 > \text{Ni} = \text{Ni-Rh} > \text{Ni-Ru}$ .

All of the catalysts tested remained active longer than we had anticipated. For Ni-Rh-A-100 (2.5% Ni, 0.5% Rh) the original  $\text{H}_2$  uptake was 19.0 micromoles/gram. Assuming 0.75 sulfur atoms adsorbed per surface Ni atom (9) and a GHSV of  $30,000 \text{ hr}^{-1}$  with 10 ppm  $\text{H}_2\text{S}$  it should take 1.0 hours to saturate the catalyst if there were no sulfur breakthrough. However, no loss of activity was observed after one hour and after 24 hours the high metal loading catalysts retained 20-30% activity. Analysis of the gas for  $\text{H}_2\text{S}$  downstream of Ni-Rh-A-100 sample revealed a gradual  $\text{H}_2\text{S}$  breakthrough. Apparently, equilibrium adsorption does not occur under these reaction conditions, possibly because of competitive adsorption by reacting species.

Figure 8 shows normalized activity plotted versus time divided by hydrogen uptake for powdered samples of 3%  $\text{Ni}/\text{Al}_2\text{O}_3$ , 20%  $\text{Ni}/\text{Al}_2\text{O}_3$ , 20%  $\text{Co}/\text{Al}_2\text{O}_3$ , 10%  $\text{Ni}/10\% \text{Co}/\text{Al}_2\text{O}_3$  and 10%  $\text{Ni}/10\% \text{MoO}_3/\text{Al}_2\text{O}_3$  tested in 99%  $\text{H}_2$ , 1%  $\text{CO}$  and 10 ppm  $\text{H}_2\text{S}$ . The results of normalizing time with respect to surface area are very interesting. The deactivation curves for 3 and 20% nickel are very nearly coincidental. The curves for 20% Ni and 20% Co are essentially the same and are represented by a single curve. The curve for Ni-Co shows slightly higher activity for values of the abscissa from 0.1 to 0.5. The activity of 10% Ni/10%  $\text{MoO}_3/\text{Al}_2\text{O}_3$ , however, is significantly higher for values of the abscissa above 0.2. Comparison of the data for 3% Ni in Figures 7 and 8 (two different reactant gas compositions (surface area of  $34.9 \text{ umoles/g}$ ) reveals that the rate of deactivation is higher for the run in the hydrogen rich reactant mixture (99%  $\text{H}_2$ ), although the two curves evidence a similar exponential decay.

Several attempts were made to regenerate the poisoned catalysts by heating them in pure  $\text{H}_2$ ,  $\text{CO}$ , air or  $\text{H}_2/\text{CO}$  mixtures. After treating catalysts in  $\text{H}_2$  at 723 K for 12-24 hours, it was possible to recover 5-15% of the original  $\text{H}_2$  uptake. In no case, however, was any methanation activity recovered. In fact, after treatment at 723 K the activity dropped to zero, even when samples were tested at elevated temperatures. Based upon our NSF investigation of sulfur adsorption (9), a surface reconstruction or phase transformation of the adsorbed sulfur to a totally inactive nickel sulfide may be occurring. This change apparently occurs to a greater extent at higher temperatures. Treatment in  $\text{H}_2$  at 523 K also resulted in further loss of activity, although samples were active when tested at high temperatures. A Ni-Co powder treated for 3 hours in  $\text{CO}$ , then 30 minutes in air followed by an 11 hour reduction in  $\text{H}_2$  at 525 K showed an increase in activity (measured at 525 K) from 0.20 to 0.37.

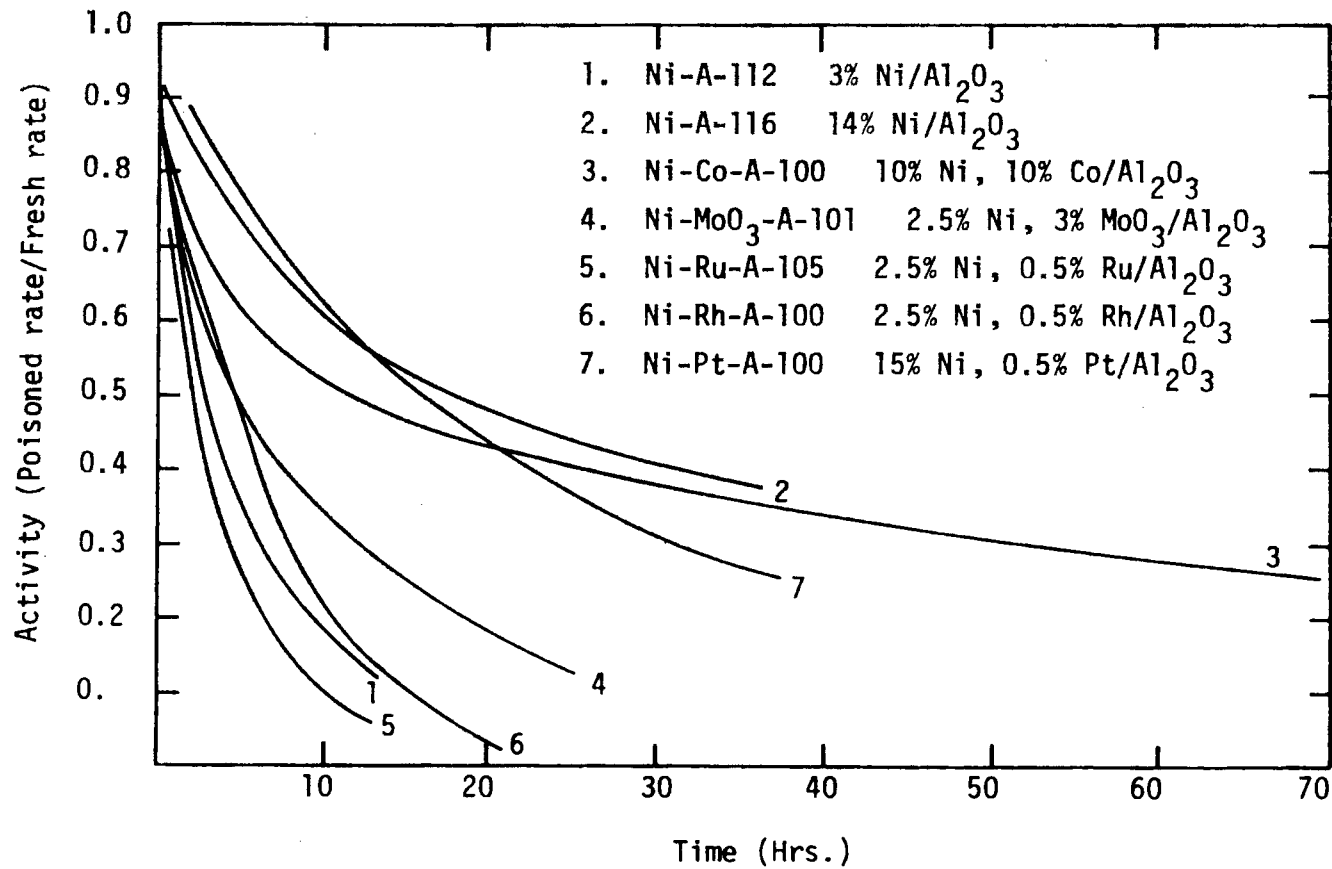


Figure 7. Smoothed Activity-Time Curves for Powdered Alumina-supported Nickel and Nickel Bimetallics during Exposure to 10 ppm  $\text{H}_2\text{S}$  in 1%  $\text{CO}$ , 4%  $\text{H}_2$ , and 95%  $\text{N}_2$  (GHSV = 30,000  $\text{hr}^{-1}$ , 100 kPa).

Table 7

Effects of In Situ H<sub>2</sub>S Poisoning on Activity of Powdered  
Alumina-Supported Nickel and Nickel Bimetallics at 523K  
(Space velocity of 30,000 hr<sup>-1</sup>; Feed: 1% CO, 4% H<sub>2</sub>, 10 ppm H<sub>2</sub>S, 95% N<sub>2</sub>)

Catalyst	Fresh Rate (Molecules/site sec)	Time to Reach <sup>a</sup> activity=1/2 (hours)	Time to Reach <sup>a</sup> activity=1/4 (hours)
Ni-A-112	10.6 x 10 <sup>-3</sup>	3	7.5
Ni-A-116	8.3	19	---
Ni-Co-A-100	10.6	12.5	70
NiMoO <sub>3</sub> -A-101	12.5	5.0	15
Ni-Ru-A-105	6.7	2	5
Ni-Rh-A-100	8.0	5.5	9
Ni-Pt-A-100	7.7	16	36

<sup>a</sup>activity = poisoned rate/fresh rate

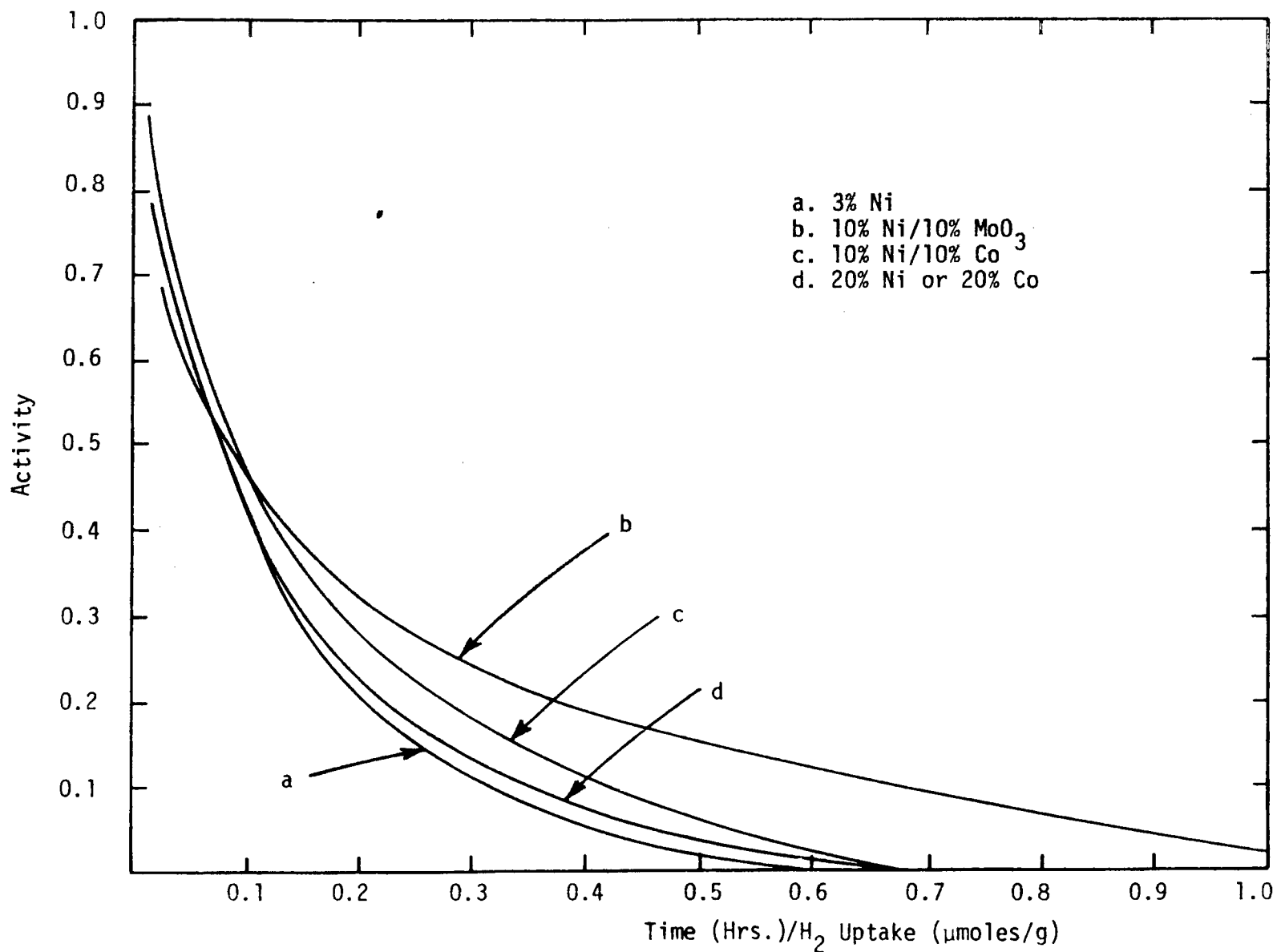


Figure 8. Activity normalized to hydrogen uptake versus time during reaction at 525 K, 110 kPa, and 30,000 hr<sup>-1</sup>. Reaction mixture = 99% H<sub>2</sub>, 1% CO, 10 ppm H<sub>2</sub>S.

b. Monolithic Catalysts. Each of the monolithic catalysts listed in Table 8 was tested at 523 K for methanation activity before, during and after exposure to 10 ppm hydrogen sulfide in the reaction mixture. The nominal catalyst compositions, fresh and poisoned turnover numbers and the time exposed to H<sub>2</sub>S are listed in Table 8. Activity, defined as the ratio of the poisoned rate to the fresh rate is plotted as a function of time in Figure 9.

Data in Table 8 and Figure 9 show that during in situ exposure to 10 ppm H<sub>2</sub>S at 523 K all of the catalysts lose approximately 40-50% of their initial activity within 20 hours. Before exposure to H<sub>2</sub>S, the order of specific activity for methane production is Ni-MoO<sub>3</sub> > Ni-Co > Ni > Ni-Ru > Ni-Pt. However, after 20 hours exposure to 10 ppm H<sub>2</sub>S at 523 K, the order of activity is Ni-MoO<sub>3</sub> > Ni > Ni-Co > Ni-Ru > Ni-Pt. Apparently, this sample of Ni-Co deactivates at a slightly faster rate than Ni.

~~Comparison of the data in Table 8 for monoliths with the data~~ in Table 7 for powder catalysts (high metal loading samples) shows that monolithic-supported Ni-Co is slightly more sulfur tolerant than the pellet-supported Ni-Co. That is, 50% activity is lost in 12.5 hours for pelleted Ni-Co compared to less than 17 hours for the monolithic Ni-Co. Pellet-supported and monolithic-supported Ni and Ni-Pt behave about the same, losing 50% activity after about 20 hours. These results are quite significant because they suggest that monolithic catalysts are at least as tolerant to sulfur poisoning as pellet catalysts and perhaps more so because these monolithic catalysts contain 30-40% less active metal by weight and have lower surface areas (lower S adsorption capacity).

Attempts to regenerate sulfur poisoned monolithic catalysts in flowing pure hydrogen met with different results than with pelleted catalysts. The monoliths heated in the presence of the reaction mixture for up to 4 hours at various temperatures between 523 and 673 K did not lose additional activity beyond that which had occurred during the poisoning test. This suggests that thin-layer (similar to eggshell in pellets) type poisoning occurs in the case of the monolithic catalysts.

### 3. Activity Measurements of Fresh and Poisoned Catalysts - Powders Compared to Pellets

Both fresh and partially sulfided samples (treated in 10 ppm H<sub>2</sub>S/H<sub>2</sub> at 723 K) of Ni-Co-A-100 (powdered form) were differentially tested at 498, 523 and 548 K at a space velocity of 100,000 hr<sup>-1</sup>. The results are shown in Table 9. Previously reported data on Ni-Co-A-100 pellets are also included. The samples were tested in the powdered form to decrease the effects of diffusional resistance and pore mouth poisoning thought possible in pellets. CO turnover numbers for the fresh powder were 2-3 times larger than those previously reported for a pelleted sample; however, the methane turnover numbers were about the same. The high percentage of CO conversion without corresponding methane or carbon dioxide production for the powder suggests that the surface composition of the powdered sample is significantly different and such as to produce a significant amount of heavy hydrocarbons.

Table 8

Effects of In Situ Poisoning on the Activities of Nickel Bimetallic Monolithic Catalysts  
with 10 ppm H<sub>2</sub>S at 523K (30,000 hr<sup>-1</sup> GHSV, 95% N<sub>2</sub>, 4% H<sub>2</sub>, 1% CO)

Catalyst	Nominal Composition	Fresh Turnover No.	Poisoning Time	Poisoned Turnover No.	Activity after Poisoning
Ni-M-117	12% Nickel, 20% alumina, 68% ceramic	23.4 x 10 <sup>-3</sup>	20	12.2 x 10 <sup>-3</sup>	0.52
Ni-Co-M-105	5.5% Nickel, 5.5% Cobalt, 18.5% alumina, 70% ceramic	25.5	17.1	10.7	0.42
Ni-MoO <sub>3</sub> -M-111	6% Nickel, 6% MoO <sub>3</sub> , 20% alumina, 68% ceramic	41.5	20.2 42.8	18.2 14.7	0.44 0.35
Ni-Pt-M-107	0.58% Platinum, 11% Nickel, 20% alumina, 68% ceramic	17.7	20.2 26.7	8.8 8.2	0.50 0.46
Ni-Ru-M-108	5.8% Nickel, 1.2% Ruthenium, 19.3% alumina, 74% ceramic	18.7	12.1 19.6	10.9 10.2	0.58 0.54

Turnover Number = molecules CH<sub>4</sub> formed per second per fresh H chemisorption site.

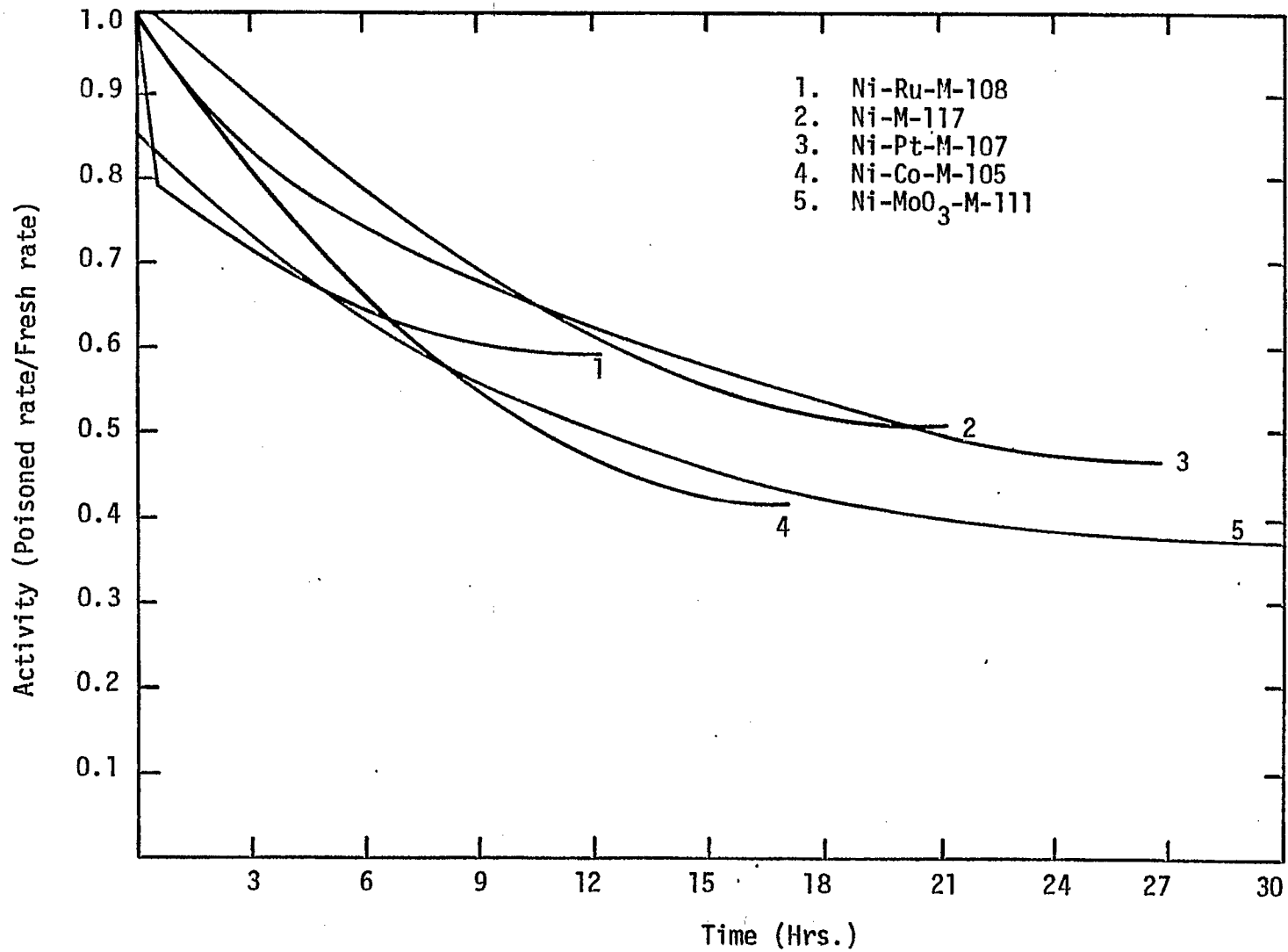


Figure 9. Smoothed Activity-Time curves for Monolithic-Supported Nickel and Nickel-Bimetallics during Exposure to 10 ppm in 1% CO, 4% H<sub>2</sub>, and 95% N<sub>2</sub> (GHSV = 30,000 hr<sup>-1</sup>, 100 kPa).

Table 9

Differential Reactor Data  
for Ni-Co-A-100 Before and After H<sub>2</sub>S Poisoning  
(100 kPa, 100,000 hr<sup>-1</sup>, 95% H<sub>2</sub>, 4% H<sub>2</sub>, 1% CO)

Catalyst	μmoles/g H <sub>2</sub> uptake	H <sub>2</sub> S poisoned uptake	% CO conversion	% Production		Yield		Rate X10 <sup>7</sup> g moles/ g cat-sec		Turnover # X10 <sup>3</sup>	
				CH <sub>4</sub>	CO <sub>2</sub>	CH <sub>4</sub>	CO <sub>2</sub>	CO	CH <sub>4</sub>	CO	CH <sub>4</sub>
Ni-Co-A-100 before poisoning	148.2		15.6	at 498 K		0.30	0.00	33.8	10.1	11.4	3.42
				4.7	0.0						
Ni-Co-A-100 Pellets	114.9		14.8	12.3	3.6	.84	.024	8.4	7.0	3.6	3.0
Ni-Co-A-100 after poisoning <sup>a,b</sup>	148.2	69.7	1.7	1.7	-0.3	1.02	-0.16	3.6	3.6	2.5	2.6
Ni-Co-A-100 before poisoning	148.2		26.0	at 523 K		.54	.04	56.5	30.6	19.0	10.3
				14.1	0.9						
Ni-Co-A-100 pellets	114.9		35.5	28.5	2.27	.80	.064	20.3	16.3	8.5	6.9
Ni-Co-A-100 after poisoning	148.2	69.7	6.2	4.2	-0.1	.87	-0.02	13.3	8.9	9.5	6.4
Ni-Co-A-100 before poisoning	148.2		50.0	at 548 K		0.61	0.15	108.4	66.2	36.6	22.4
				30.5	7.3						
Ni-Co-A-100 pellets				Not Available							
Ni-Co-A-100 after poisoning	148.2	69.7	9.9	8.3	0.7	.84	.07	21.2	17.84	15.2	12.8

<sup>a</sup> poisoned in fixed bed in flowing H<sub>2</sub> and 10 ppm H<sub>2</sub>S until approximately 50% poisoned

<sup>b</sup> reactant stream contained approximately .01% CO<sub>2</sub>

Perhaps this is an effect of Fischer-Tropsch "conditioning" which occurs more rapidly in small catalyst particles. The nickel-cobalt powder was prepared from the same batch as the pelleted sample, but it was bulk reduced at a different time possibly under slightly different conditions. The higher  $H_2$  uptake suggests that its surface properties (i.e. surface composition) could be different from the earlier batch. This renders the comparison between the pellets and powder difficult and perhaps inconclusive. Also some  $CO_2$  was found to be in the reactant stream during the differential test of the sulfided powder which alters the test conditions somewhat and accounts for the negative values of  $CO_2$  production, mainly artifacts of the calculation.

Nevertheless, the methane turnover number data for the powdered catalyst before and after poisoning reveal a significant decrease in specific activity of the remaining sites after poisoning, in contrast to the increase observed previously for the pellet supported catalyst (3). Hence, the data suggest that catalyst geometry plays an important role in the poisoning process and these data are indeed consistent with a pore mouth or shell type poisoning model.

Partly because of these unusual results and the obviously nonuniform nature of  $H_2S$  poisoning, a further series of tests was conducted for alumina supported Ni, Ni-Co, and Co Catalysts of high metal loading (14-20%) in powder form in which the samples were poisoned in a uniform manner by 24 hour exposure to 10 ppm  $H_2S/H_2$  in a fluidized bed reactor. A schematic of the fluidized bed reactor is shown in Figure 10. The methane turnover number data obtained before and after poisoning at high space velocities and low conversions are shown in Table 10. Poisoned site activity ratios (PSAR values), ratios of the turnover number of the poisoned to that of the fresh catalyst are also listed. That the PSAR values for the uniformly poisoned catalysts are significantly less than one (on the order of 0.5) suggests that adsorbed  $H_2S$  interacts with the nickel surface to deactivate more than one nickel site for every adsorbed sulfur atom and/or restructures the surface such that the remaining sites are less active. The larger methane turnover numbers and PSAR values for Ni-Co compared to Ni and Co, an obvious synergistic effect, provide indirect evidence of an intimate bimetallic interaction or perhaps an alloying effect.

It should be mentioned here that the nickel and nickel-cobalt catalysts were observed to be relatively stable over a period of 30-60 minutes during which time 5-6 chromatographic samples were obtained. The  $Co/Al_2O_3$  powder, however, was observed to lose activity with time particularly at the higher temperature (525 K) and especially after exposure to  $H_2S$ . For example, the poisoned sample lost 45% of its initial activity at 525 K over a period of about 45 minutes. This deactivation is possibly a result of high molecular weight hydrocarbons depositing on the surface, since supported Co is known to be active for Fischer-Tropsch Synthesis. Because this deactivation was not observed in the testing of the same catalyst in pellet form at lower space velocities, the deactivation phenomenon may be dependent upon catalyst geometry and upon space velocity.

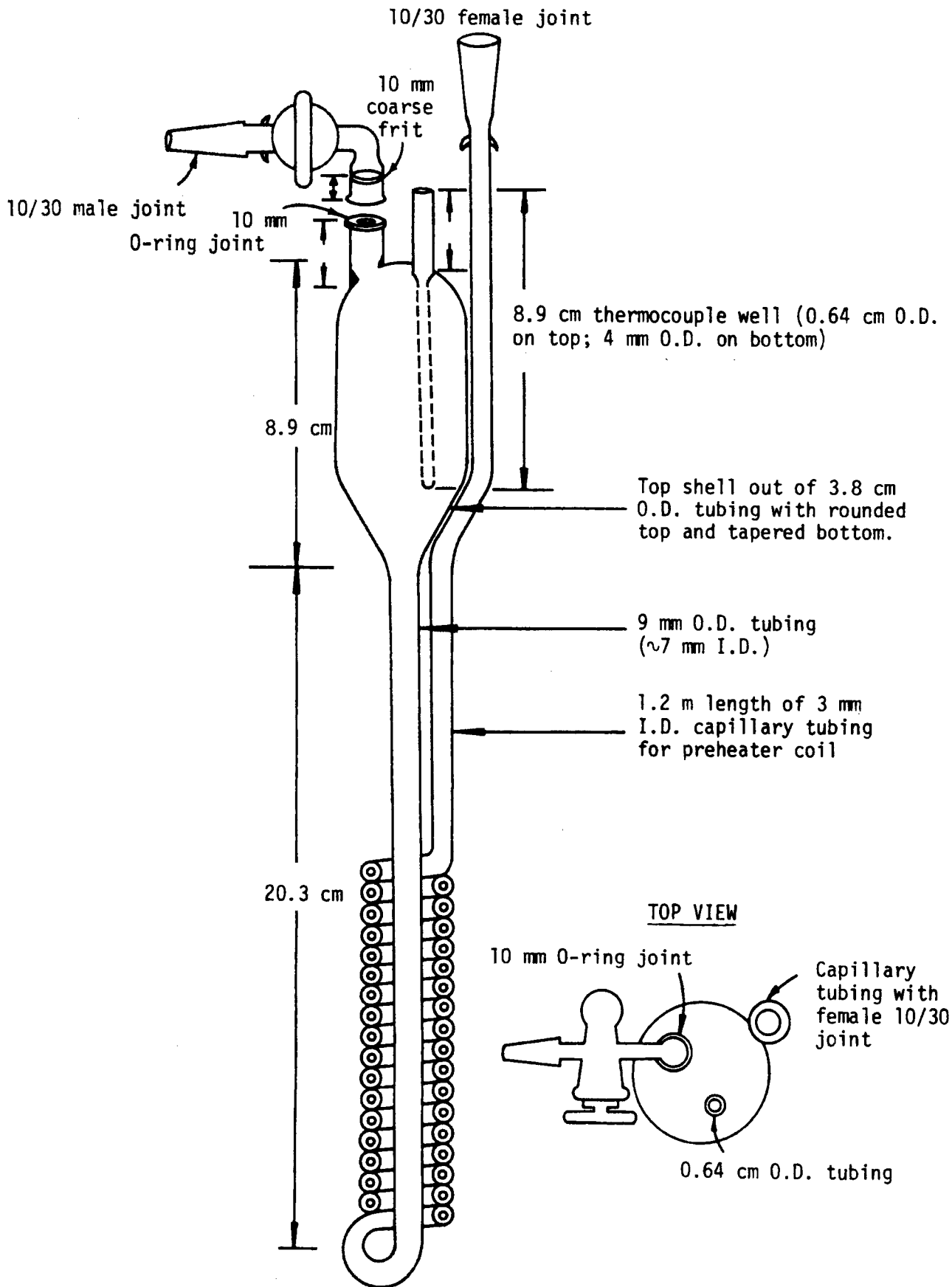


Figure 10. Fluidized Bed Reactor.

Table 10

Specific Activity Data<sup>a</sup> Before and After Exposure<sup>b</sup> to 10ppm H<sub>2</sub>S  
of Alumina-Supported Ni, Ni-Co and Co in Powder Form

<u>Catalyst</u>	<u>% CO Conversion</u>	<u>% CH<sub>4</sub> Yield<sup>c</sup></u>	<u>CH<sub>4</sub> Turnover No. X10<sup>3</sup> (sec<sup>-1</sup>)</u>	<u>Poisoned Site Activity Ratio<sup>d</sup></u>
<u>At 500 K</u>				
<u>Ni-A-116 (14% Ni)</u>				
fresh	4.04	71.5	2.4	0.42
poisoned	2.69	61.4	1.0	
<u>Ni-Co-A-100 (10% Ni, 10% Co)</u>				
fresh	4.46	61.2	6.0	0.68
poisoned	2.80	81.8	4.1	
<u>Co-A-100 (20% Co)</u>				
fresh	2.01 <sup>e</sup>	61.2	3.8	0.53
poisoned	2.26 <sup>f</sup>	55.8	2.0	
<u>At 525 K</u>				
<u>Ni-A-116 (14% Ni)</u>				
fresh	9.85	83.6	6.9	0.40
poisoned	6.28	74.2	2.8	
<u>Ni-Co-A-100 (10% Ni, 10% Co)</u>				
fresh	8.60	85.6	16.1	0.83
poisoned	8.44	89.7	13.4	
<u>Co-A-100 (20% Co)</u>				
fresh	5.81 <sup>e</sup>	56.9	10.3	0.34
poisoned	3.25 <sup>f</sup>	65.2	3.5	

<sup>a</sup>At 140 kPa, a space velocity of about 100,000 hr<sup>-1</sup> in a gas mixture containing 1% CO, 4% H<sub>2</sub>, 95% N<sub>2</sub>.

<sup>b</sup>Exposure to 10ppm H<sub>2</sub>S in a fluidized bed over a period of several hours sufficient to poison about 50% of the surface.

<sup>c</sup>Methane yield is the fraction of converted CO which is transformed to methane.

<sup>d</sup>Turnover number for the poisoned divided by that for the fresh catalyst.

<sup>e</sup>Space velocity = 100,000 hr<sup>-1</sup>

<sup>f</sup>Space velocity = 38,000 hr<sup>-1</sup>.

#### 4. Support Geometry Tests:

Conversion vs. temperature tests were conducted on three nickel on alumina monolithic catalysts: Ni-AM-101, Ni-AM-102 and Ni-AM-201. The test conditions included a space velocity of  $30,000 \text{ hr}^{-1}$ , a reaction mixture of 95%  $\text{N}_2$ , 4%  $\text{H}_2$  and 1%  $\text{CO}$  and a pressure of 140 kPa. These tests are summarized in Table 11 along with the results of some previously reported tests (3). Figure 11 is representative of the results of these tests.

Table 11 also shows how the nickel on alumina monolith catalysts compare with  $\text{Al}_2\text{O}_3$  - washcoated monolithic catalysts previously tested in this laboratory. It appears as though the nickel on alumina catalysts are less selective towards methane than are the alumina-coated monoliths. The difference in selectivity may be due to diffusional effects.

Also from Table 11, it can be seen that the rates per gram catalyst for the nickel on alumina monoliths are much larger than the rates of the other catalysts at 598 K. This can be explained by the smaller catalyst density of the alumina monolith relative to the cordierite monolithic support.

As part of the support geometry testing under Task 2, several monolithic and beaded catalysts were tested under high temperature and hopefully mass transfer limiting conditions to see if support geometry had an effect in these reaction regimes.

Each of the catalysts tested (see Table 12) was characterized by determination of geometrical surface area (GSA). This catalyst characteristic is the criterion by which monolithic and pelleted catalysts can be compared in mass transfer limiting regimes. The geometrical surface area (GSA) is the exterior surface area of the catalyst implied by the geometry of the catalyst support and is reported as  $\text{cm}^2$  surface area/ $\text{cm}^3$  catalyst volume. The method of determining GSA has been reported earlier (7).

Conversion vs. temperature tests were conducted at 140 kPa and  $50,000 \text{ hr}^{-1}$ , using a reactant gas containing 1%  $\text{CO}$ , 4%  $\text{H}_2$ , and 95%  $\text{N}_2$ . The temperature varied from 450 to 750 K, however, the catalysts were compared at 700 K since that temperature was nearest the maximum  $\text{CO}$  conversion for all the catalysts. Each data value in Table 12 represents the average of data obtained for 3-4 identical samples of each geometry.

On the basis of moles of  $\text{CO}$  converted per gram of catalyst per second, a comparison of the data for the Torvex monoliths shows that the catalysts with the higher GSA also have the higher reaction rate. This indicates that for monoliths the higher the GSA the higher the reaction rate that can be expected. In comparison to the Celcor monoliths the  $40.80/\text{cm}^2$  Torvex monoliths have slightly but significantly higher rates of reaction although these two catalysts have nearly the same GSA. This difference in activity is accounted for by Hegedus (11) who shows that according to mass transfer considerations the hexagonal monolith channels should give better activity than the square

Table 11

Temperature Conversion Tests for Monolithic Catalysts  
 GHSV = 30,000 hr<sup>-1</sup>; Reactant Composition: 95% N<sub>2</sub>, 4% H<sub>2</sub>, 1% CO; 140 kPa

Catalyst <sup>a</sup>	Temperature for CO Conversion of		At 95% CO Conversion		% CO converted to CH <sub>4</sub>	At 325°C Rate of CH <sub>4</sub> Formation (moles/gram-sec x 10 <sup>7</sup> )
	50%	95%	CH <sub>4</sub>	CO <sub>2</sub>		
a. Monoliths having 31.0 square channels per square cm						
Ni-AM-101 <sup>b</sup>	265	310	73	14	78	80
Ni-AM-102 <sup>b</sup>	270	320	77	10	78	74
Ni-M-151 <sup>c</sup>	245	295	93	6	93	36
Ni-M-154 <sup>c</sup>	260	310	83	5	93	37
b. Monoliths having 36.6 triangular channels per square cm						
Ni-AM-201 <sup>b</sup>	265	305	80	11	86	71
Ni-M-250 <sup>c</sup>	250	320	87	7	86	44
Ni-M-252 <sup>c</sup>	250	300	86	10	92	47
Ni-M-254 <sup>c</sup>	255	300	83	10	91	46

<sup>a</sup>For compositions see Table 3.

<sup>b</sup>AM refers to a pure alumina monolith support.

<sup>c</sup>Previously reported catalysts (3), nickel impregnated on alumina layer on cordierite monolith catalyst support.

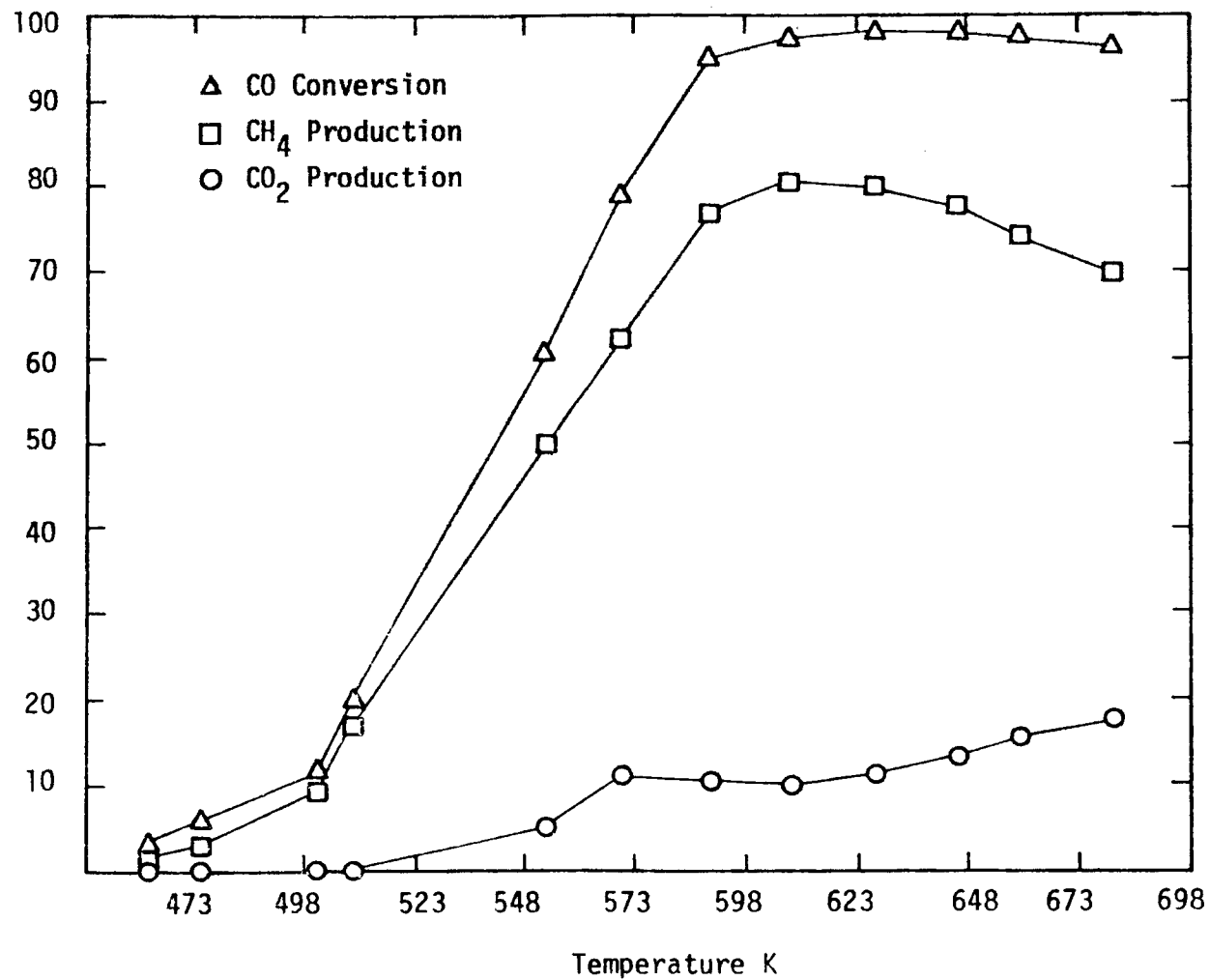


Figure 11. Conversion vs. temperature for Ni-AM-201 (140 kPa, GHSV=30,000 hr<sup>-1</sup>).

Table 12

Comparison of Geometrical Surface Area and Reaction Rates  
 [140 kPa, GHSV = 50,000 hr<sup>-1</sup>, 700 K, 1% CO, 4% H<sub>2</sub>, 95% N<sub>2</sub>]

<u>Catalyst</u>	<u>GSA</u> <sup>1</sup>	<u>wt.</u>	Rate per gram x10 <sup>7</sup>		Rate per volume x10 <sup>7</sup>	
			(mole/g-cat.-sec.)		(moles/cm <sup>3</sup> -cat.-sec.)	
			<u>CO</u>	<u>CH<sub>4</sub></u>	<u>CO</u>	<u>CH<sub>4</sub></u>
Beads (0.32 cm diam.)	8.7	2.451	94.3	59.9	36.6	23.3
Celcor 46.5 □/cm <sup>2</sup> 10 % Alumina	17.8	4.620	79.7	54.9	58.1	40.1
Torvex 40.8 ○/cm <sup>2</sup> Dupont Alumina Coat	16.6	4.048	94.7	64.5	60.8	41.4
40.8 ○/cm <sup>2</sup> Cat. Lab. Alumina Coat	16.3	4.159	91.2	63.7	60.2	42.1
10.7 ○/cm <sup>2</sup> DuPont Alumina Coat	8.9	5.079	67.9	45.3	54.7	36.5
10.7 ○/cm <sup>2</sup> Cat. Lab. Alumina Coat	9.2	5.322	66.6	44.4	56.3	37.5

<sup>1</sup>GSA is cm<sup>2</sup> exterior surface area/cm<sup>3</sup> bulk volume of catalyst.

monolith channels. On a rate/gram basis a comparison of the monoliths and beads shows a different result. Even though the beads have a smaller GSA than the monoliths, the rate of CO conversion in the pellets is as high as the best rate seen for the monoliths. However, this is mainly a result of the high density of the monolith body.

Indeed, on the basis of moles of CO converted per volume of catalyst per second, a comparison of the monoliths and beads shows significantly different results. That is monolithic supported catalysts evidence substantially higher rates/volume than the beaded catalyst. In fact, the monoliths with high GSA show rates of CO conversion nearly twice the volume of the beads. Table 12 shows that the same trends that are seen in the rate of CO conversion are also seen in the rate of CH<sub>4</sub> production. These results indicate that it would take nearly twice the volume of beads (or pellets) to convert a given amount of CO to CH<sub>4</sub> as it would monoliths. Thus, the use of monolith supported catalysts would enable the size of methanation reactors to be reduced significantly. Moreover, a monolithic reactor could be operated efficiently at substantially higher space velocities than beads or pellets at a fraction of the pressure drop.

Mass transfer coefficients were calculated for monoliths and pellets to see if the experiments were actually in the mass transfer limiting regime (see Table 13). The experimental values were calculated according to:

$$k_m = r\rho M/aC_A$$

where  $k_m$  is the mass transfer in cm/sec,  $r$  is the rate in g-moles/g-cat-sec,  $\rho$  is the bulk density,  $M$  is the molecular weight of carbon monoxide,  $a$  is the GSA in cm<sup>2</sup>/cm<sup>3</sup> and  $C_A$  is the log mean concentration of CO in g/cm<sup>3</sup>. The theoretical values of  $k_m$  for monoliths were calculated according to the method of Hegedus (11):

$$k_m = (D/2R) B (1 + .095 (4R^2G/\rho DL))^{0.45}$$

where  $D$  is the diffusivity of CO,  $R$  is the hydraulic radius,  $B$  is the limiting Sherwood number for fully developed laminar flow,  $G$  is the feed flux in g/cm<sup>2</sup>-sec,  $\rho$  is the bulk density and  $L$  is the monolith channel length. The theoretical values of  $k_m$  for pellets were based on the correlation of Petrovic and Thodos (12).

From Table 13, one can see that these experiments were carried out in the mass transfer influenced regime, but that mass transfer was not the rate limiting step. Since diffusivity and, hence, the mass transfer coefficient are inversely dependent upon pressure, the calculated mass transfer coefficient should be about a factor of 10 less at 1000 kPa, suggesting that truly mass-transfer-limiting conditions will obtain under these conditions.

During the last quarter, some of the same catalysts tested were tested at 1000 kPa. The results presented in Tables 14 and 15 are only preliminary findings, but the same trends observed at the lower pressure are also in evidence although the effects are not nearly

Table 13

## Experimental and Theoretical Mass Transfer Coefficients

(140 kPa, GHSV = 50,000 hr<sup>-1</sup>, 700 K, 1% CO, 4% H<sub>2</sub>, 95% N<sub>2</sub>)

	Experimental $k_m$ (cm/sec)	Theoretical $k_m$ (cm/sec)
Beads (0.32 cm diam.)	2.71	14.8
Celcor 46.5 □/cm <sup>2</sup> 10% Alumina	6.43	20.1
Torvex 40.8 ○/cm <sup>2</sup> Dupont Alumina-Coated	8.09	21.1
40.8 ○/cm <sup>2</sup> Cat. Lab Alumina Coat	8.52	21.8
10.7 ○/cm <sup>2</sup> Dupont Alumina Coat	6.94	10.6
10.7 ○/cm <sup>2</sup> Cat. Lab Alumina Coat	7.61	10.5

Table 14

Comparison of Geometrical Surface Area and Reaction Rates  
 [1000 kPa, GHSV=50,000 hr<sup>-1</sup>, 700 K, 1% CO, 4% H<sub>2</sub>, 95% N<sub>2</sub>]

Catalyst	CAT Number	GSA <sup>1</sup>	Wt.	H <sub>2</sub> uptake μmoles/g	Rate per gram X10 <sup>7</sup> (mole/g-cat.-sec.)		Rate per <sub>3</sub> volume X10 <sup>7</sup> (mole/cm <sup>3</sup> -cat.-sec.)	
					CO	CH <sub>4</sub>	CO	CH <sub>4</sub>
Beads 0.32 cm diam.	Ni-A-121	8.7	2.58g	73.9	140.2	116.0	57.41	47.5
Celcor 46.5 □/cm <sup>2</sup>	Ni-M-356	17.8	4.2064	26.1	94.86	86.44	63.29	57.71
Celcor 46.5 □/cm <sup>2</sup>	Ni-M-357	17.8	4.2283	31.5	87.50	74.09	58.72	49.73
Celcor 31 □/cm <sup>2</sup>	Ni-M-156		4.3921	46.0	83.85	74.81	58.46	52.15
Torvex 40.8 ○/cm <sup>2</sup>	Ni-TM-110	16.6	3.9338	36.8	94.6	82.0	59.07	51.20
Torvex 10.7 ○/cm <sup>2</sup>	Ni-TM-350	9.2	5.4847	45.2	64.15	57.76	55.85	50.28

<sup>1</sup>GSA is cm<sup>2</sup> exterior surface area/cm<sup>3</sup> bulk volume of catalyst.

Table 15

Comparison of Geometrical Surface Area and Conversion  
 Production and Selectivity  
 [1000 kPa, GHSV=50,000 hr<sup>-1</sup>, 700 K, 1% CO, 4% H<sub>2</sub>, 95% N<sub>2</sub>]

<u>Catalyst</u>	<u>CAT Code</u>	<u>GSA</u>	<u>Uptake</u> <u>μmoles H<sub>2</sub>/g</u>	<u>wt.</u>	<u>% Conversion</u> <u>CO</u>	<u>% Production</u>		<u>% Yield</u>	
						<u>CH<sub>4</sub></u>	<u>CO<sub>2</sub></u>	<u>CH<sub>4</sub></u>	<u>CO<sub>2</sub></u>
Beads 0.32 cm diam.	Ni-A-121	8.7	73.9	2.58	90.3	73.8	11.2	82.0	12.0
Celcor 46.5 □/cm <sup>2</sup>	Ni-M-356	17.8	26.1	4.2064	99.8	90.94	7.31	91.1	7.3
Celcor 46.5 □/cm <sup>2</sup>	Ni-M-357	17.8	31.5	4.2283	92.25	78.1	10.43	84.7	11.3
Celcor 31 □/cm <sup>2</sup>	Ni-M-156		46.0	4.3921	97.04	86.57	13.01	89.2	13.4
Torvex 40.8 ○/cm <sup>2</sup>	Ni-TM-110	16.6	36.8	3.9338	96.46	83.71	13.0	86.8	13.5
Torvex 10.7 ○/cm <sup>2</sup>	Ni-TM-350	9.2	45.2	5.4847	93.19	83.19	11.78	90.0	12.6

so dramatic. Again, the catalysts are compared at 700 K which may in this case introduce some discrepancies. The conversion for the pellets reaches a maximum at this temperature, but this is not the case for the monoliths (see Figure 12). Many of the monolithic catalysts tested attained 100% conversion at much lower temperatures and then began to decrease in activity as the temperature increased. It is not entirely clear whether this is a mass transfer effect or a simple equilibrium effect. It is clear, however, that comparisons at high pressure need to be made at lower temperatures and even higher space velocities! Nevertheless, as can be seen in Table 14, the percent CO conversion at 700 K and the selectivity to  $\text{CH}_4$  production are higher for monoliths in all instances than for the pelleted catalyst. The rates per volume in Table 15 are also generally higher for the monoliths than for the pellets. These values are for single catalyst samples. During the next quarter, more samples will be run to test for reproducibility and mass transfer coefficients will be calculated to insure that we are indeed in the mass transfer limiting region at lower temperatures (e.g. 600 K). In addition, several monolith geometries not previously tested will be run at 1 atm, since at 10 atm the catalysts are obviously too active to enable a reasonable comparison even at a space velocity as high as  $50,000 \text{ hr}^{-1}$ .

### Task 3: Kinetic Studies

Construction of the high pressure mixed flow system has been completed. Five runs have been made to check the equipment. Temperature control and equilibration have proven to be the main concerns. The temperature inside the Berty reactor and the heating rate have been found to be functions of reactor pressure, impeller speed and flow rate. Higher flow rates give a more uniform temperature in reactor, while increasing reactor pressure and impeller speed increases temperature equilibration and heating rates.

Several reactor tests with catalyst pellets in the Berty reactor have been made during the last quarter. The gas chromatograph is presently set up for analysis of both reactants and products and the high pressure reactor system is operational. The Haskell gas compressor has been used to prepare gas mixtures up to 14,000 kPa.

### Task 4: Degradation Studies

#### 1. Upper Operating Temperature Limit Tests

During the past two quarters, upper operating temperature limit (thermal degradation) tests were performed on high loading alumina-supported Ni, Ni-Co, Ni-MoO<sub>3</sub> and Ni-Pt. Also, Ni on nickel aluminate and commercially prepared G-87P and MC-100 were tested. The tests were performed at 2500 kPa and a space velocity of  $30,000 \text{ hr}^{-1}$ . The reactant gas was 64%  $\text{CH}_4$ , 16% Ar, 14%  $\text{H}_2$ , 4% CO, 2%  $\text{CO}_2$ . Graphs of these runs are shown in Figures 13, 14 and 15. During these tests, care was taken to avoid temperature spikes when the reactant gases were added to the reduced catalyst. Thus, Argon was added first and

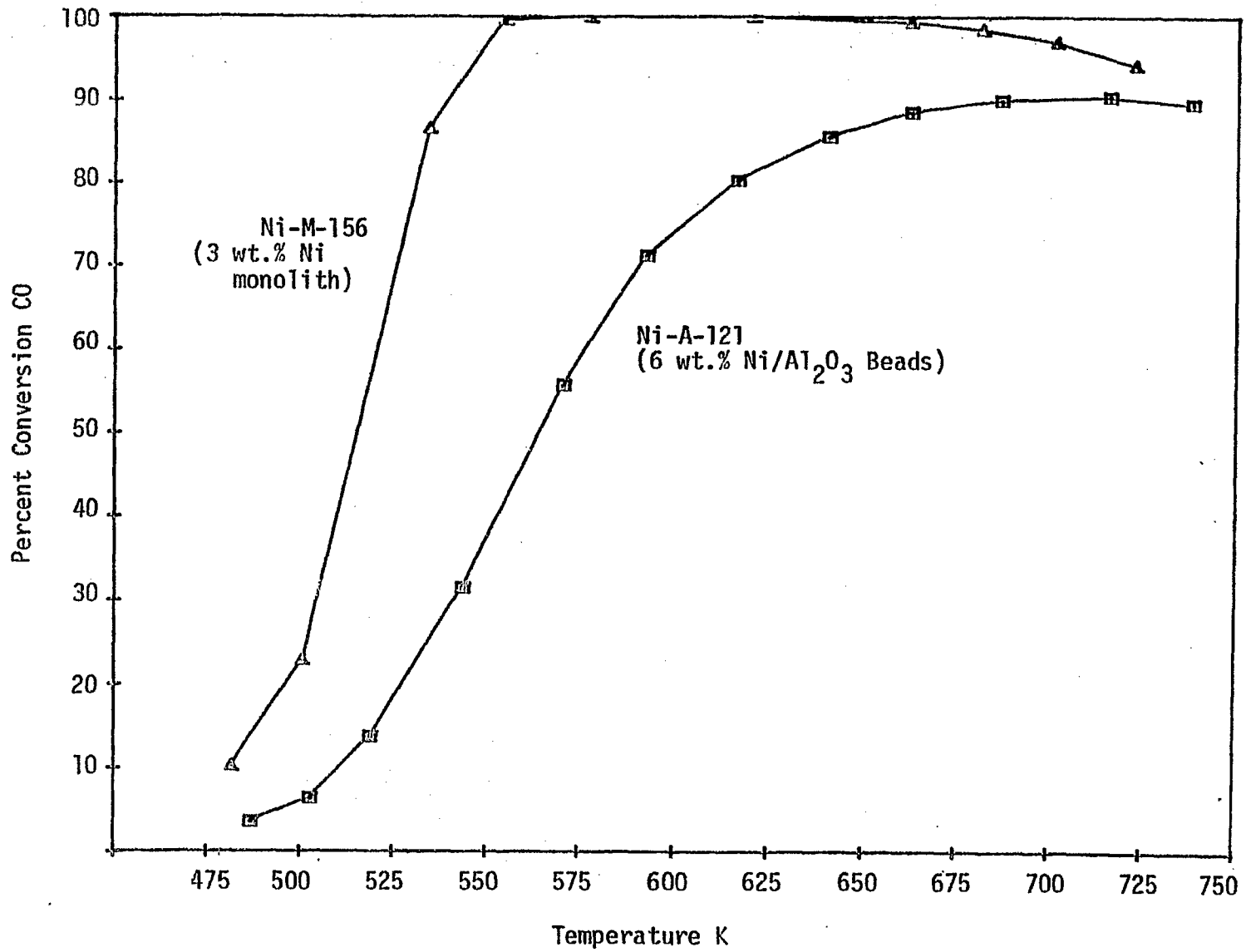


Figure 12. CO conversion vs. Temperature for Ni-M-156 and Ni-A-121 (1000 kPa, GHSV=30,000 hr<sup>-1</sup>)

CH<sub>4</sub> was added next. Then, as the temperature settled down to 525 K, the CO, CO<sub>2</sub> and H<sub>2</sub> were added gradually to full flow.

In Figure 13, the conversion of CO (to all products) is shown with respect to temperature. The equilibrium conversion as calculated by the Edward's Thermochemical Program is higher than the actual conversions experienced in the upper temperature limit runs. At peak conversion the order of catalyst activity was Ni > Ni-Co > Ni/NiAl<sub>2</sub>O<sub>4</sub> > Ni-MoO<sub>3</sub>. A second run on Ni-A-122 (20% Ni) was made to investigate the deactivation at higher temperatures. Deactivation did not become rapid until ≈823 K. The catalyst still converted 50% of the reactant CO at 886 K. These catalysts did better than those reported by Lee (12) where most of the commercial catalysts deactivated at 783 K.

During the last quarter, we tested two commercially prepared catalysts G-87P (Girdler) and MC-100 (Union Carbide). A comparison of these tests with Run B for Ni-A-122 is shown in Figure 14. The Ni-A-122 performed better than the commercial catalysts at higher temperatures (>750 K). This may be because Run B was started at a higher temperature or because the catalysts prepared in this laboratory are more thermally stable than commercially prepared methanation catalysts.

In Figure 15, the results of three more tests are shown. At higher temperatures, the order of activity is Ni-Pt > Ni or NiAl<sub>2</sub>O<sub>4</sub> > Ni monolith. The good performance of Ni-Pt reinforces earlier work in this laboratory (3, 5) that showed that Ni-Pt was more resistant to carbon deposition than other nickel catalyst combinations. NiAl<sub>2</sub>O<sub>4</sub> Run B showed improved activity over Run A (see Figure 13). The catalyst sample for Run B was reduced 6 hours in flowing H<sub>2</sub>, rather than just 2 hours.

Figure 16 shows conversion of CO to CH<sub>4</sub> versus temperature for several of the same catalysts. The presence of 64% methane inerts requires the subtraction of two nearly equal numbers resulting in roundoff error. Therefore, these calculations are made using a carbon balance over CO, CH<sub>4</sub> and CO<sub>2</sub>. The assumption that negligible carbon is deposited appears to be very good except above 773 K. At that temperature, a run on a blank sample gave 20% conversion of CO to CH<sub>4</sub>. This anomalous value was an artifact of the calculation and the confidence interval for values of CH<sub>4</sub> production is about 50%. The roundoff error does not occur in CO conversion calculation. Above 773 K in the test without steam, the carbon balance assumption also affects the CO conversion calculation to the extent of approximately 10%.

## 2. Upper Operating Temperature Tests With Steam

Upper operating temperature limit tests were also made with a gas composition of 64% CH<sub>4</sub>, 12% Ar, 14% H<sub>2</sub>, 4% CO, 2% CO<sub>2</sub> and 4% H<sub>2</sub>O (steam) on the following catalysts: Ni-A-122, Ni-Co-A-103, Ni-Pt-A-101, Ni-M-180, Ni-NAL-100, G87-P and MC-100. Ni-MoO<sub>3</sub>-A-105 was also tested, but the steam content was only 2%. The test conditions were again 2500 kPa and a space velocity of approximately 30,000. The steam tests required addition of a condensor and trap for removal

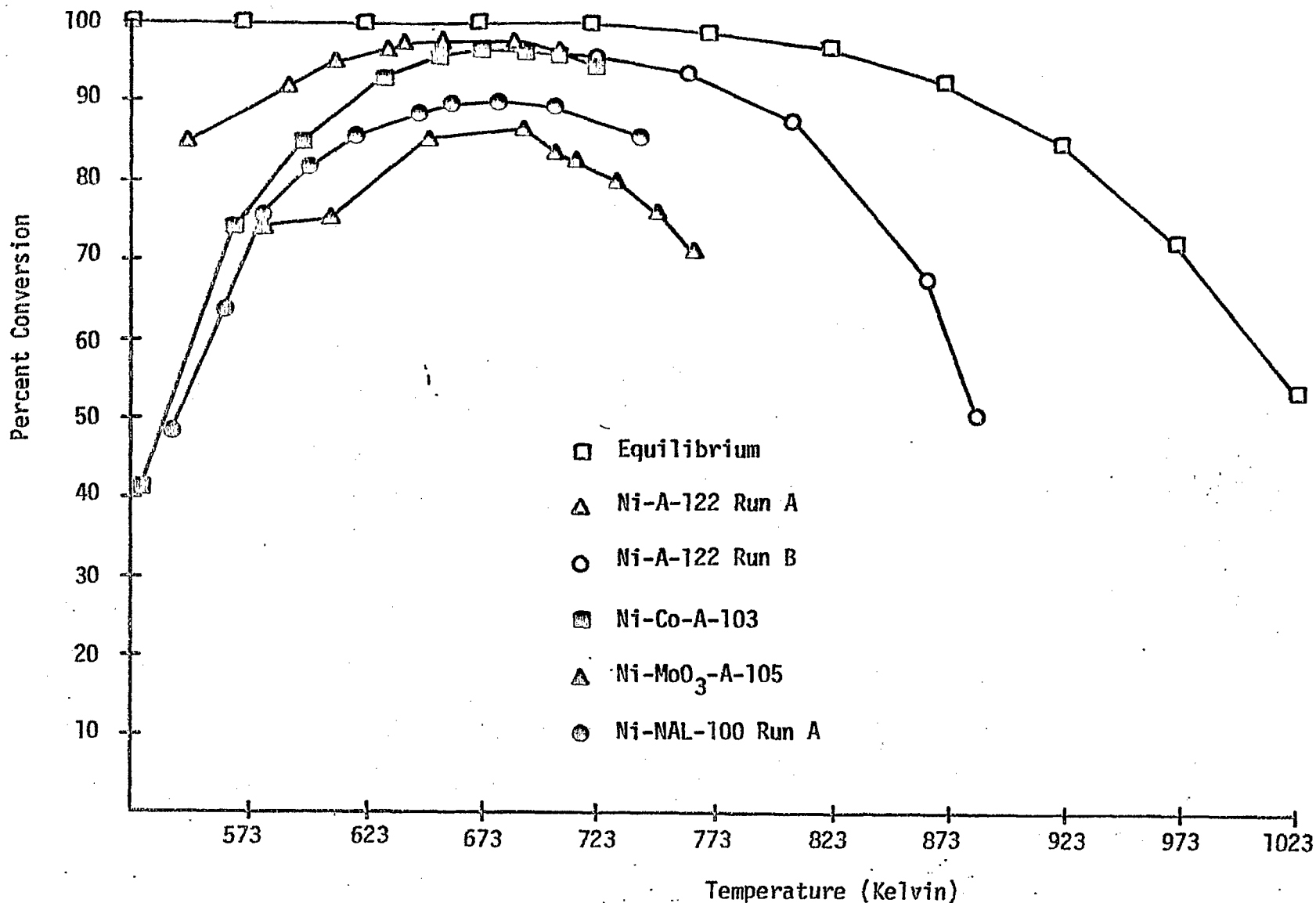


Figure 13. Conversion of CO (overall) vs. Temperature for High Loading Catalysts at 2500 kPa, GHSV=30,000 hr<sup>-1</sup>, and Reaction Mixture Containing 64% CH<sub>4</sub>, 16% Ar, 14% H<sub>2</sub>, 4% CO, and 2% CO<sub>2</sub>.

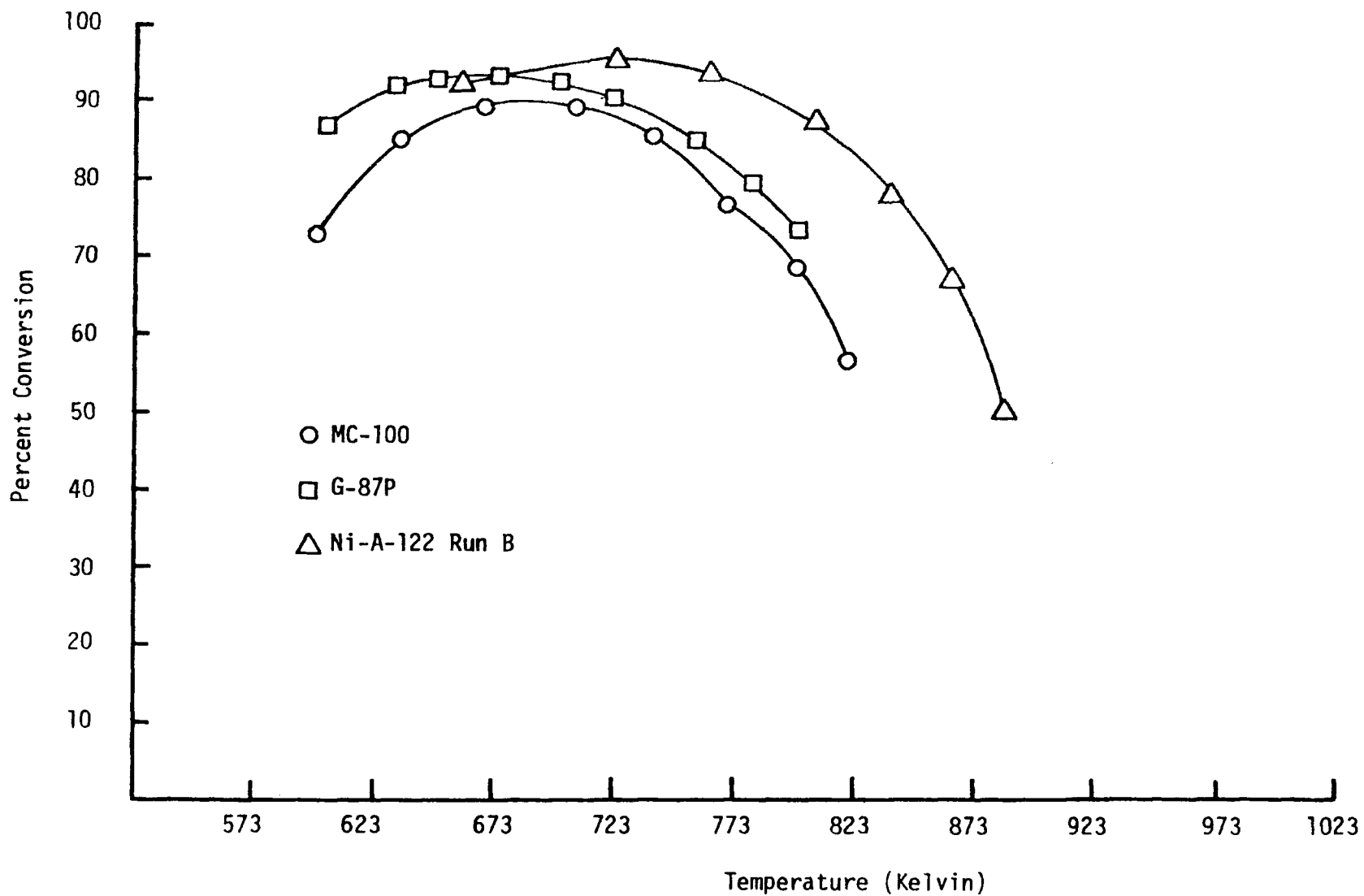


Figure 14. Conversion of CO (overall) vs. Temperature for High Loading Catalysts at 2500 kPa, GHSV=30,000 hr<sup>-1</sup>, and Reaction Mixture Containing 64% CH<sub>4</sub>, 16% Ar, 14% H<sub>2</sub>, 4% CO, and 2% CO<sub>2</sub>.

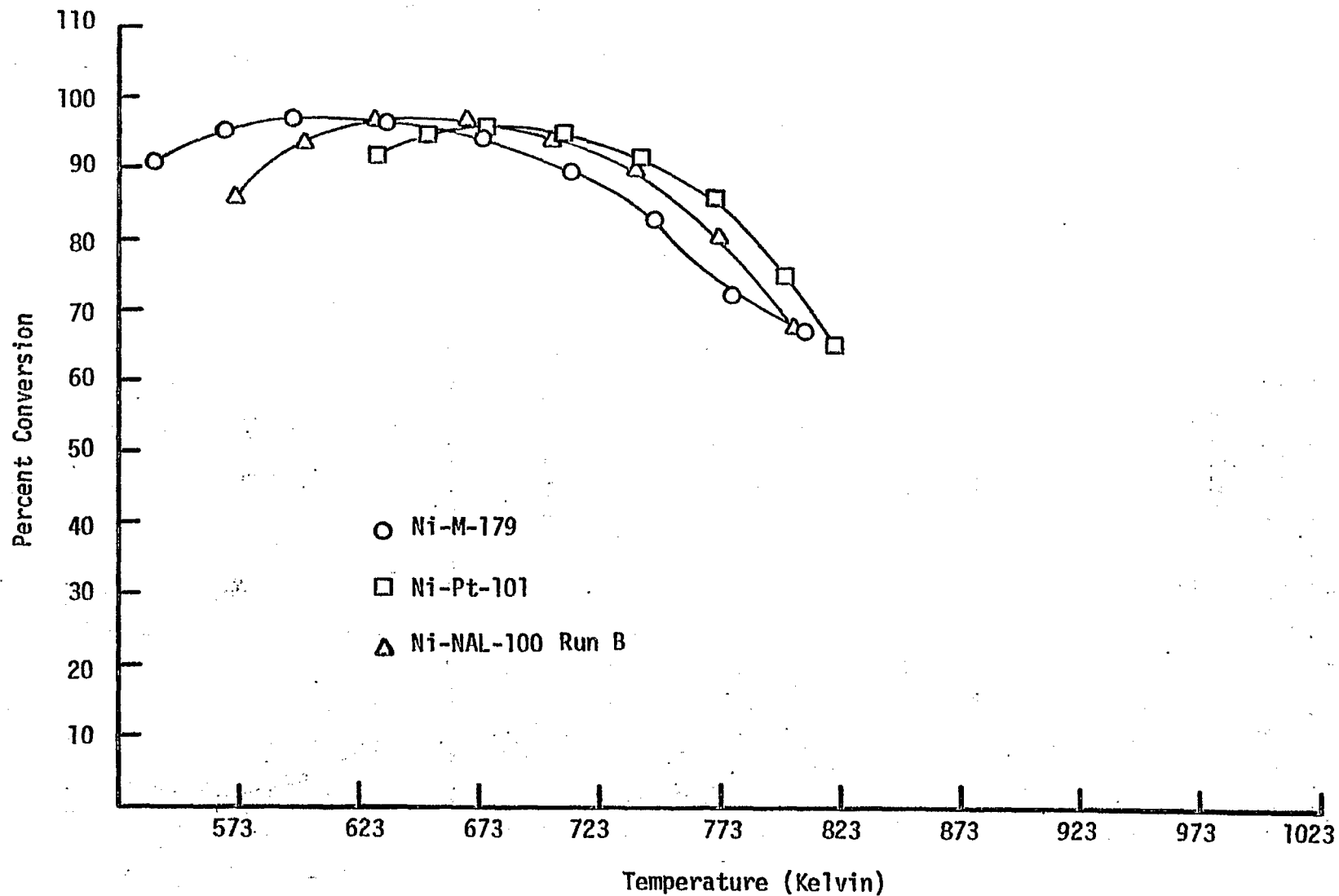


Figure 15. Conversion of CO (overall) vs. Temperature for High Loading Catalysts at 2500 kPa, GHSV=30,000 hr<sup>-1</sup>, and Reaction Mixture Containing 64% CH<sub>4</sub>, 16% Ar, 14% H<sub>2</sub>, 4% CO, and 2% CO<sub>2</sub>.

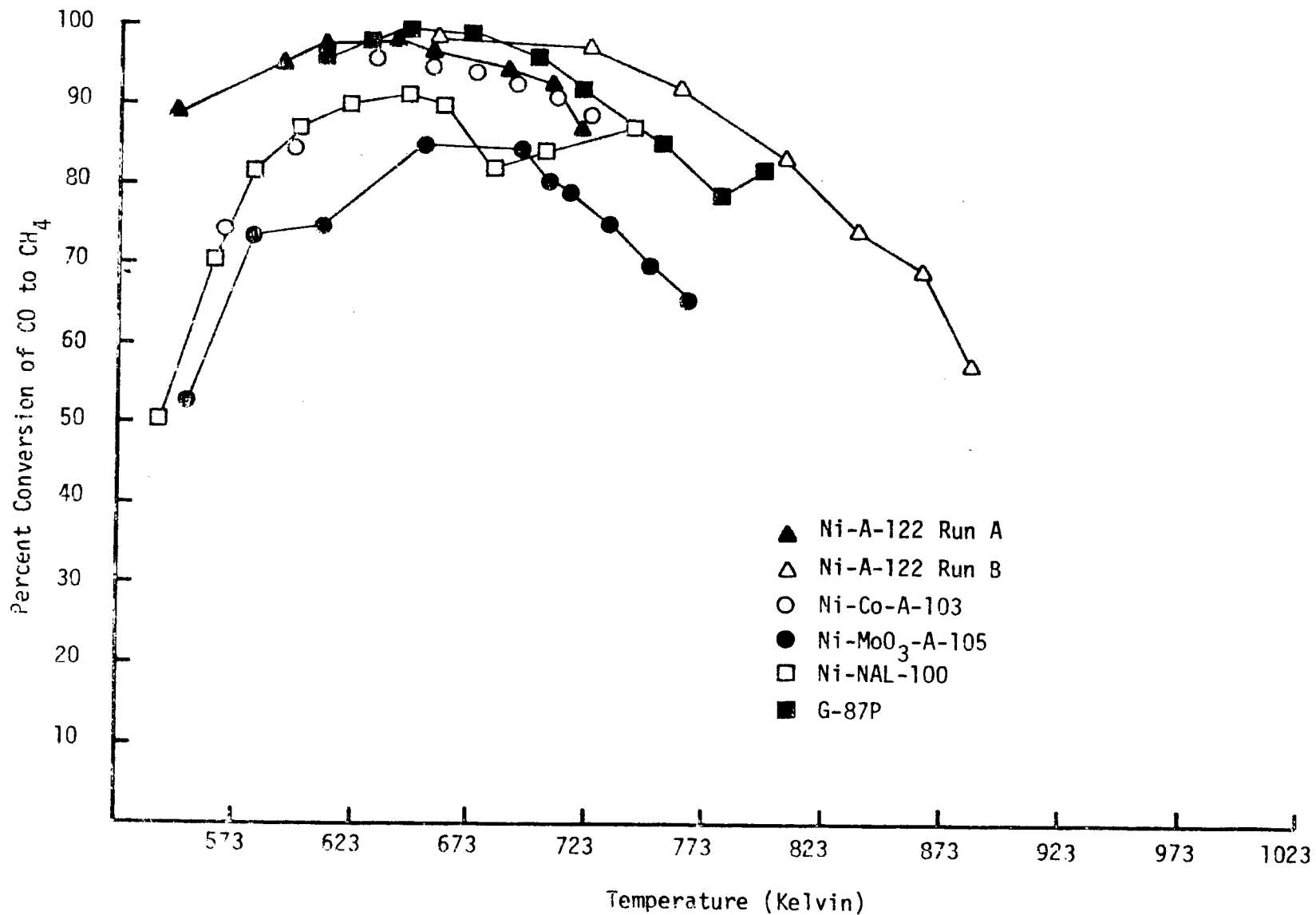


Figure 16. Conversion of CO to CH<sub>4</sub> vs. Temperature for High Loading Catalysts at 2500 kPa, GHSV=30,000 hr<sup>-1</sup>, and Reaction Mixture Containing 64% CH<sub>4</sub>, 16% Ar, 14% H<sub>2</sub>, 4% CO, and 2% CO<sub>2</sub>.

of water before sampling. Graphs of results from these tests are shown in Figures 17 and 18.

Figures 17 and 18 show CO conversion versus temperature. Generally, the order of activity is Ni > Ni-Pt > Ni-NAL = Ni-Co = MC-100 > G87P > Ni monolith > Ni-MoO<sub>3</sub>. In both these figures CO conversion drops off about as rapidly as it did in the runs without steam. The addition of steam should inhibit carbon formation. So, it appears that the activity drop off is due to something other than carbon deposition.

In Figure 19, the percent conversion of CO to CH<sub>4</sub> is given versus temperature. The maximum conversion is reached between 623 and 673 K. Then, the CH<sub>4</sub> conversion decreases rapidly until it becomes negative. At this point, CH<sub>4</sub> is reformed to CO and CO<sub>2</sub>.

#### Task 5: Technical Interaction and Technology Transfer

On October 10, 1977, Dr. Bartholomew, the Principal Investigator, visited the University of Kentucky and the Institute for Mining and Minerals Research where he presented a seminar on our methanation catalysis research. Arrangements were made with Phil Reucroft, Professor of Materials Science, and John Hahn, Associate Director of the Institute to exchange samples and provide each other with data on nickel catalysts. The Institute will perform ESCA and x-ray diffraction measurements on well-characterized nickel catalysts prepared at BYU and the BYU Catalysis Laboratory agreed to measure methanation activities of the commercial catalysts under study at the Institute.

The Principal Investigator also attended the Fall Meeting of the California Catalysis Society held in Pasadena on October 20-21 and presented a paper on sintering of Ni/Al<sub>2</sub>O<sub>3</sub> catalysts. The meeting also provided opportunities to communicate with methanation researchers on recent developments, especially in the areas of sulfur poisoning and carbon deposition. Arrangements were made with Bob Lewis at Chevron to perform ESCA work on our Ni-MoO<sub>3</sub> catalyst. Dr. Lewis has the capability of reducing the catalysts in situ before running the spectra - a feature which is not yet available at the University of Utah where most of our work has been done.

Dr. Bartholomew and 8 students, Jay Butler, Erek Erekson, Mark Jeffery, Donald Mustard, Edward Sughrue, John Watkins, Art Uken and Gordon Weatherbee attended the 3rd Rocky Mountain Fuel Symposium held February 10-11 in Albuquerque. Dr. Bartholomew participated as symposium chairman while Mr. Weatherbee presented a paper entitled, "In situ Poisoning by Sulfur of Nickel and Nickel Bimetallic Methanation Catalysts." The Rocky Mountain Fuel Society was successfully organized and officers for the new organization were elected. Dr. Bartholomew was elected to the Board of Directors.

On December 30, Mr. Ed Sughrue visited the research lab of Dr. William Thompson at the University of Idaho at Moscow. The purpose of the visit was to examine the "Berty" high pressure constant volume

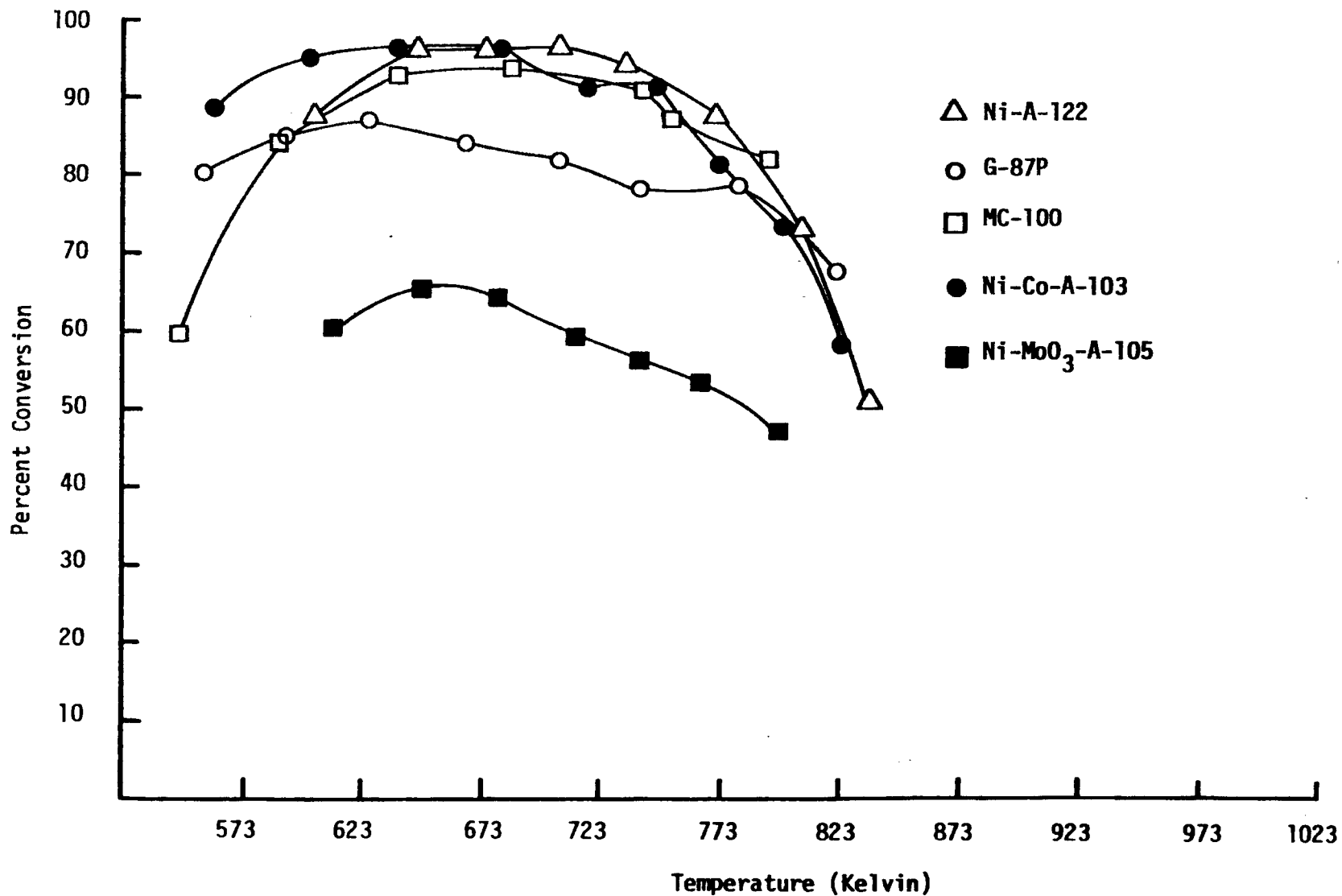


Figure 17. Conversion of CO (overall) vs. Temperature for High Loading Catalysts at 2500 kPa, GHSV=30,000 hr<sup>-1</sup>, and Reaction Mixture Containing 64% CH<sub>4</sub>, 12% Ar, 14% H<sub>2</sub>, 4% CO, 2% CO<sub>2</sub>, and 4% H<sub>2</sub>O.

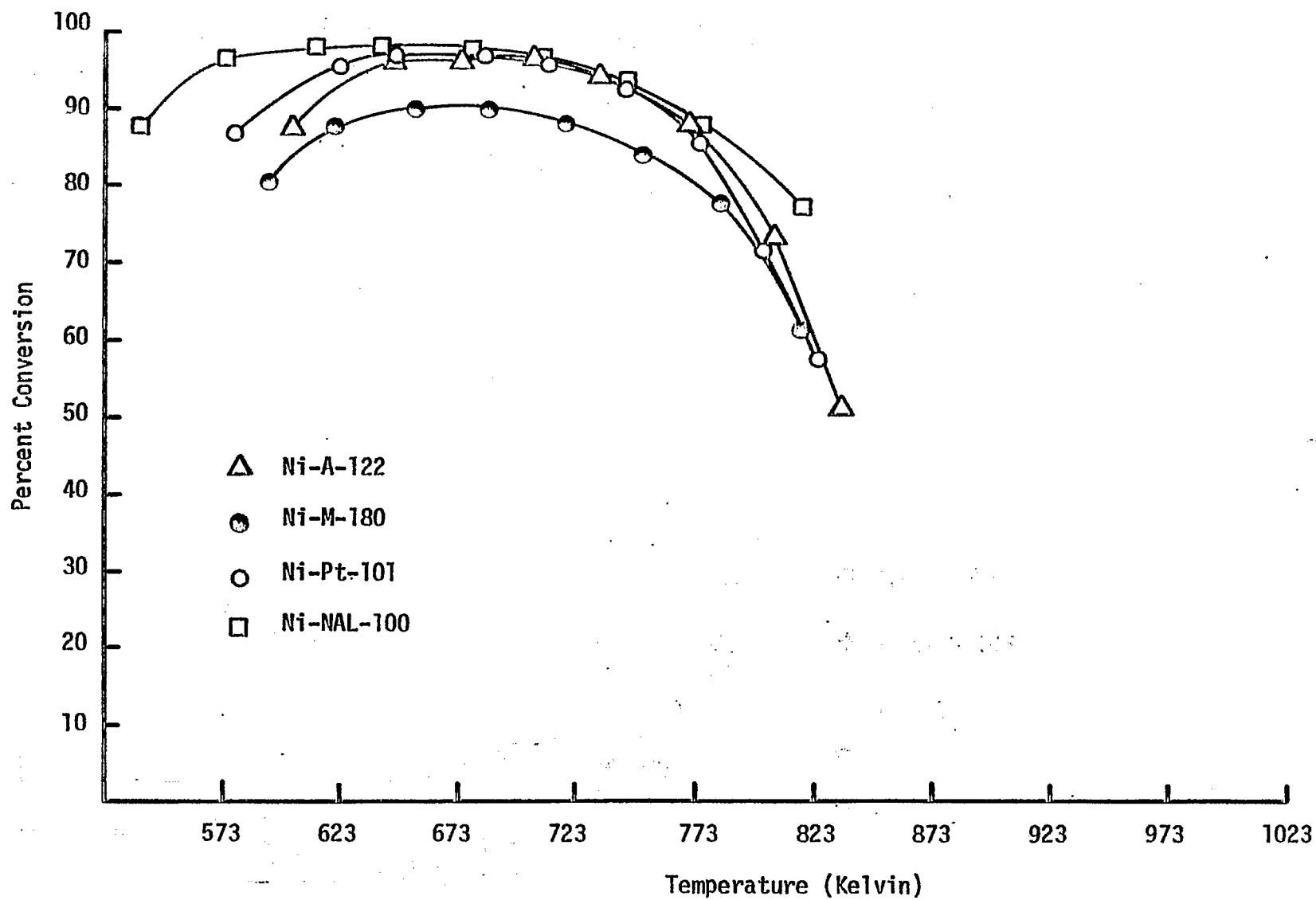


Figure 18. Conversion of CO (overall) vs. Temperature for High Loading Catalysts at 2500 kPa, GHSV=30,000 hr<sup>-1</sup>, and Reaction Mixture Containing 64% CH<sub>4</sub>, 12% Ar, 14% H<sub>2</sub>, 4% CO, 2% CO<sub>2</sub>, and 4% H<sub>2</sub>O.

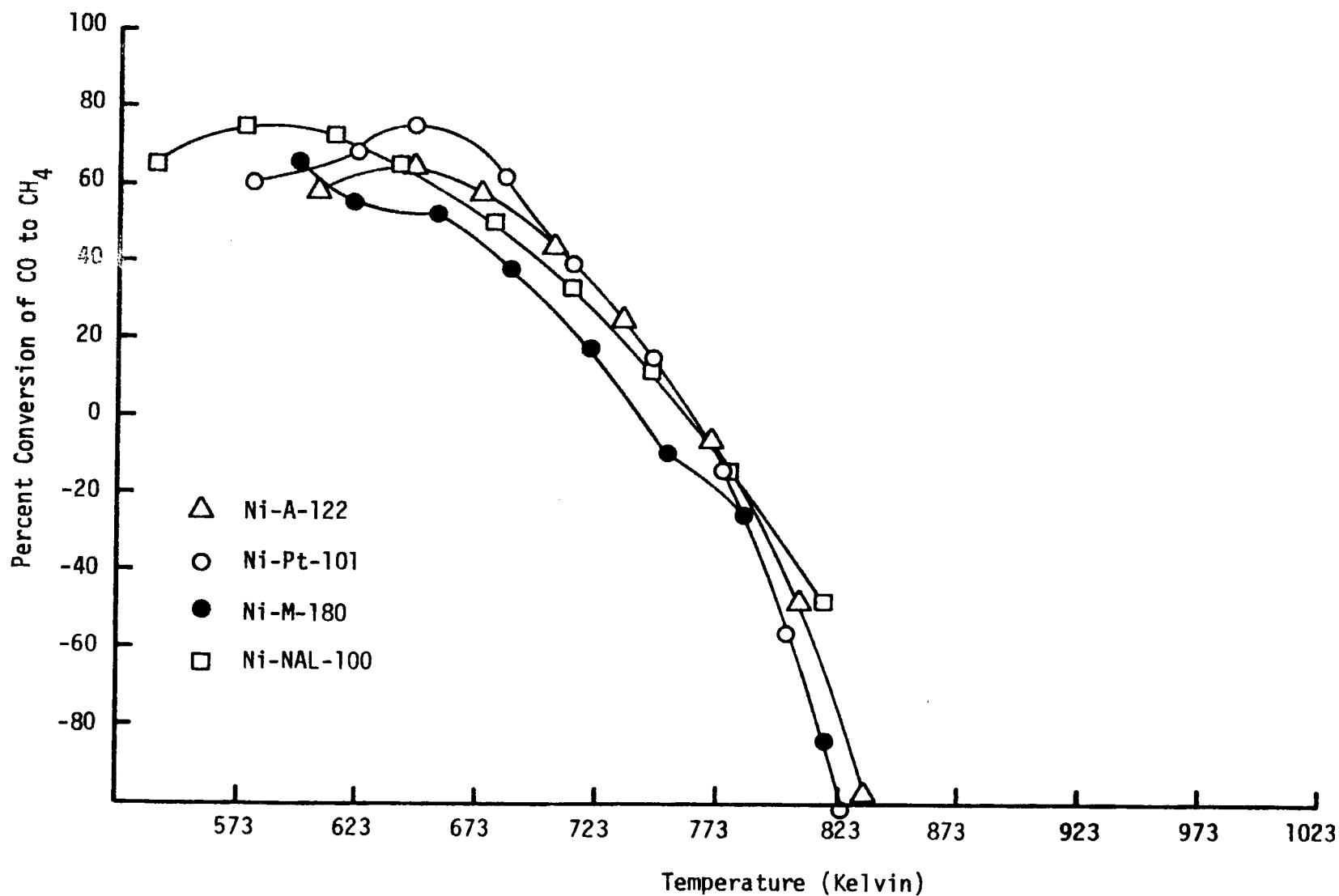


Figure 19. Conversion of CO to CH<sub>4</sub> vs. Temperature for High Loading Catalysts at 2500 kPa, GHSV=30,000 hr<sup>-1</sup>, and Reaction Mixture Containing 64% CH<sub>4</sub>, 12% Ar, 14% H<sub>2</sub>, 4% CO, 2% CO<sub>2</sub>, and 4% H<sub>2</sub>O.

mixed flow systems built by Dr. Thompson. Instruction concerning installation, maintenance and application of the "Berty" system for university lab research was received. Safety measures were also discussed in depth.

On March 17, Dr. Robert Ference of the Climax Molybdenum Co. of Michigan, visited our laboratory where he presented a seminar dealing with applications of molybdenum catalysts and toured our facilities. We are currently in close communication with Dr. Ference regarding the preparation and testing of Ni-MoO<sub>3</sub> catalysts.

On May 3 the principal investigator, Dr. Bartholomew, visited by invitation the Division of Applied Photochemistry at Los Alamos Scientific Laboratory (New Mexico), toured selected laboratories and presented a seminar "The Future of Catalysis." Several stimulating discussions with scientists of the AP Division focused on the possible applications of Laser Technology to the study of catalysts and catalytic reactions.

On May 15th he visited the Norton Chemical Company in Akron, Ohio where he presented a seminar on CO and H<sub>2</sub> adsorption on nickel and toured the company's R & D facilities. The following day he attended a meeting of the D-32 Catalyst Committee of the American Society for Testing and Materials and participated in the preparation of standard techniques for measuring metal areas of Ni/Al<sub>2</sub>O<sub>3</sub> and Pt/Al<sub>2</sub>O<sub>3</sub> catalysts using hydrogen adsorption. Discussions with Dr. Robert Farrauto (Engelhard) and Dr. Ruth Haines (NBS) provided useful feedback on several catalyst characterization problems.

The following week Dr. Bartholomew attended a conference on Catalyst Deactivation and Poisoning held May 24-26 at the Lawrence Berkeley Laboratory in Berkeley, California and presented a paper on "H<sub>2</sub>S Poisoning of Supported Nickel and Nickel Bimetallic Catalysts," based on our ERDA-DOE supported research. In discussions following the talk quite specific feedback was obtained in regard to our sulfur poisoning work.

Dr. Bartholomew also visited with scientists and engineers at the Climax Molybdenum Company of Michigan on June 5th, presented a seminar on "Molybdenum Based Methanation Catalysts" and toured their research and development facilities. Discussions focused on the NiMoO<sub>3</sub> catalysts prepared at BYU and at Climax which are more active and sulfur resistant than nickel catalysts and the results of our tests on several fluidized methanation catalysts (some prepared at Climax) for Bituminous Coal Research.

The following day (June 6) he met with Paul Scott and Mike Biallis of DOE-Fossil energy to review progress on the current project and to discuss ideas for possible follow on work. In the afternoon he visited Dee Stevenson of DOE-Office of Energy Research to obtain feedback on concepts for a new proposal.

On June 7th, Dr. Bartholomew presented a paper "Bimetallic Methanation Catalysts" at the 85th National Meeting of the American Institute of Chemical Engineers in Philadelphia. This presentation was a summary of activity and deactivation studies conducted over the past year in behalf of ERDA and DOE. There were two other very interesting papers presented at the same session--a paper by Professor John Butt of Northwestern dealing with hydrocarbon synthesis (characterization, activity and selectivity studies) on Fe and Ni-Fe alloys and a paper by Professor Albert Vannice of Penn State on metal support interactions in the Ni/TiO<sub>2</sub> system and their effects on methanation activity and selectivity.

Dr. Bartholomew was invited to participate in a workshop sponsored by the National Science Foundation held June 22 and 23 at the University of Maryland. The purpose of the workshop was to assess the current status of fundamental research in catalysis and to define future basic research needs, priorities, and promising directions. Dr. Bartholomew assisted in the formulation of guidelines and directives in metal catalysis and catalyst degradation.

Our research effort with monolithic catalysts recently received national attention in a science/technology concentrate appearing in the June 19th issue of Chemical and Engineering News. This article refers to our recent work which shows that monolithic catalysts are more active and possibly more cost effective than pellet catalysts for methanation.

Erek Erekson attended the DOE/Fossil Energy contractors conference on August 23 in Lexington, Kentucky. He presented a talk reviewing our progress in methanation catalyst research and participated in some important discussions with other researchers in catalysis.

On September 25, Dr. Bartholomew visited Gulf Research Company in Pittsburgh where he toured facilities and presented a seminar on "Sulfur Poisoning of Methanation Catalysts," based mainly on our DOE supported work.

During the next quarter, he plans to give a similar presentation at the 71st Annual Meeting of the AIChE in Miami. Several publications based on this study are also in preparation.

### Miscellaneous

During the past year, two students (Mr. George A. Jarvi and Mr. Gordon D. Weatherbee) have completed Master's Theses in conjunction with this study. Mr. Jarvi successfully completed his M.S. work in February and accepted employment with the Institute of Gas Technology. Mr. Weatherbee is in the process of completing his M.S. requirements while beginning Ph.D. work. Mr. Erek Erekson and Mr. Edward Sughrue are continuing their Ph.D. studies in connection with this contract work. Five graduate and three undergraduate students have contributed to this research project during the past year.

#### IV. CONCLUSIONS

1. Support geometry tests of several monolithic and pelleted catalysts show that monolithic catalysts are clearly more active than pellets on a rate/volume of catalyst basis. Also, the percent yield of methane is higher for the monolithic catalysts. These tests were conducted at high conversions under conditions similar to those in a commercial reactor.

2. Uniform H<sub>2</sub>S poisoning of alumina-supported Ni, Ni-Co and Co powders in a fluidized cell and subsequent activity testing show that specific activities are significantly higher for Ni-Co. This synergistic effect supports the hypothesis that the activity of the Ni-Co catalyst is due to the presence of an alloy. Other H<sub>2</sub>S poisoning tests of Ni-Co/Al<sub>2</sub>O<sub>3</sub> powders compared with pellets provide evidence for a shell-type poisoning model.

3. In situ H<sub>2</sub>S poisoning (10 ppm) of pelleted catalysts shows the order of poisoning resistance to be Ni > Ni-Co > Ni-Pt for high loading samples and Ni-MoO<sub>3</sub> > Ni = Ni-Rh > Ni-Ru for low loading samples. The gradual breakthrough of H<sub>2</sub>S in in situ runs suggests that non-equilibrium H<sub>2</sub>S adsorption occurs under reaction conditions. H<sub>2</sub>S adsorption apparently competes with the adsorption of reacting species and does not reach equilibrium. Attempts to regenerate the in situ poisoned catalysts with H<sub>2</sub> and H<sub>2</sub>-CO mixtures failed. During treatment with H<sub>2</sub> or H<sub>2</sub>-CO, there is probably a surface reconstruction or a phase transformation to a totally inactive metal sulfide. Treatment of poisoned catalysts with O<sub>2</sub> was successful in partially restoring catalyst activity.

4. During in situ H<sub>2</sub>S poisoning (10 ppm) of monolithic catalysts, the order of activity is Ni-MoO<sub>3</sub> > Ni > Ni-Co > Ni-Ru > Ni-Pt. Monoliths are at least as tolerant to H<sub>2</sub>S poisoning as pelleted catalysts. Attempts to regenerate poisoned monoliths in H<sub>2</sub> and H<sub>2</sub>-CO mixtures were likewise unsuccessful.

5. Carbon deposition tests for monolithic catalysts reveal the order of resistance to carbon deactivation to be Ni-Pt > Ni-Co > Ni-Ru > Ni > Ni-MoO<sub>3</sub> in qualitative agreement with previously reported tests for pelleted catalysts. Flowing H<sub>2</sub> regenerates a portion of the catalyst activity after carbon deactivation.

6. H<sub>2</sub> chemisorption uptakes on alumina monolithic supported Ni indicate better metal dispersions than for alumina-coated cordierite supported Ni. Activity tests show alumina monolithic catalysts to have higher rates/gram but lower rates/catalyst volume and lower selectivities to methane.

7. In high temperature tests with a reactant stream similar to a commercial methanation recycle reactor high loading Ni-A-122 retains activity to 823 K (550°C). The temperature of maximum conversion for high loading Ni, Ni-Co, Ni-MoO<sub>3</sub> and Ni on nickel aluminate in similar tests is near 723 K (450°C). Similar tests with steam added to the reactant gas show that carbon deposition is not the only factor causing deactivation and that reactant CH<sub>4</sub> can be reformed to CO and CO<sub>2</sub> at high temperatures in the presence of steam.

8. Nickel carbonyl formation after CO chemisorption at room temperature is significant. Also, CO uptakes on nickel catalysts vary greatly with titration temperature and sample history, while H<sub>2</sub> uptakes before and after CO adsorptions do not vary.

9. Electron micrographs of an alumina support blank show that in some cases there is not sufficient contrast between the support and metal particles to enable unambiguous determination of metal crystallite size distributions. Possible improvements in technique are being investigated.

10. In discussing and presenting the research supported by this contract, we have encountered considerable interest in three main aspects of our work. These three areas appear to have the greatest potential at this point for contributing to either the science or technology of catalysis and fossil fuel conversion:

a. Monolithic-supported catalysts: Monolithic catalysts are significantly more active and selective for methane production at high space velocities. We believe it would be possible to maintain high conversions of CO at space velocities as high as 50,000-100,000 hr<sup>-1</sup>, 2-3 times the allowable throughput for fixed pellet beds because of pressure drop considerations. We are currently working with industrial representatives to have these tested on a larger scale.

b. Ni-Co and Ni-MoO<sub>3</sub> Bimetallics: Both our Ni-Co and Ni-MoO<sub>3</sub> catalysts are more active and sulfur tolerant than nickel in methanation of CO. We have at least indirect evidence at this point of bimetallic interactions which account for this synergistic behavior. Ni-Co and Ni-MoO<sub>3</sub> catalysts are now under commercial development, and in at least one instance, we know that our work has influenced this development.

c. Poisoning and Carbon Deposition Studies: There is considerable interest in our studies of poisoning by H<sub>2</sub>S and fouling by carbon deposition during reaction on nickel and nickel bimetallics because these same problems are encountered on the very similar catalysts in a number of other important catalytic processes including hydrogenation reactions, fuel cell catalysis and hydrocarbon synthesis.

## V. REFERENCES

1. M. Greyson, "Methanation" in "Catalysts" Vol. IV., ed. P.H. Emmett, Reinhold Pub. Corp., New York (1956).
2. G.A. Mills and F.W. Steffgen, "Catalytic Methanation," *Catalysis Reviews* 8, 159 (1973).
3. C.H. Bartholomew, "Alloy Catalysts with Monolith Supports for Methanation of Coal-Derived Gases," Final Technical Progress Report FE-1790-9 (ERDA), (Sept. 6, 1977).
4. J.R. Katzer, private communication.
5. C.H. Bartholomew, "Alloy Catalysts with Monolith Supports for Methanation of Coal-Derived Gases," Final Technical Progress Report FE-2729-1 (DOE), (Jan. 5, 1978).
6. C.H. Bartholomew, "Alloy Catalysts with Monolith Supports for Methanation of Coal-Derived Gases," Final Technical Progress Report FE-2729-2 (DOE), (April 5, 1978).
7. C.H. Bartholomew, "Alloy Catalysts with Monolith Supports for Methanation of Coal-Derived Gases," Final Technical Progress Report FE-2729-3, (July 5, 1978).
8. S.E. Wanke and P.C. Flynn, "The Sintering of Supported Metal Catalysts," *Catal. Rev. - Sci. Eng.* 12, 93 (1975).
9. C.H. Bartholomew, J.L. Oliphant, R.W. Fowler and R.B. Pannell, *Journal of Catalysis* 51, 229 (1978).
10. L.L. Hegedus, "Effects of Channel Geometry on the Performance of Catalytic Monoliths," Symposium on Catalytic Approaches to Environmental Control, American Chemical Society, Division of Petroleum Chemistry, Chicago Meeting, (August 26, 1973).
11. IGT Process Research Division, "Hygas: 1972 to 1974, Pipeline Gas from Coal-Hydrogenation," Interim report No. 1, ERDA (July 1975).
12. C.N. Satterfield, "Mass Transfer in Heterogenous Catlysis," MIT Press, p. 82 (1970).

## **SATISFACTION GUARANTEED**

**NTIS strives to provide quality products, reliable service, and fast delivery. Please contact us for a replacement within 30 days if the item you receive is defective or if we have made an error in filling your order.**

▲ **E-mail: [info@ntis.gov](mailto:info@ntis.gov)**  
▲ **Phone: 1-888-584-8332 or (703)605-6050**

# **Reproduced by NTIS**

National Technical Information Service  
Springfield, VA 22161

***This report was printed specifically for your order from nearly 3 million titles available in our collection.***

For economy and efficiency, NTIS does not maintain stock of its vast collection of technical reports. Rather, most documents are custom reproduced for each order. Documents that are not in electronic format are reproduced from master archival copies and are the best possible reproductions available.

Occasionally, older master materials may reproduce portions of documents that are not fully legible. If you have questions concerning this document or any order you have placed with NTIS, please call our Customer Service Department at (703) 605-6050.

## **About NTIS**

NTIS collects scientific, technical, engineering, and related business information – then organizes, maintains, and disseminates that information in a variety of formats – including electronic download, online access, CD-ROM, magnetic tape, diskette, multimedia, microfiche and paper.

The NTIS collection of nearly 3 million titles includes reports describing research conducted or sponsored by federal agencies and their contractors; statistical and business information; U.S. military publications; multimedia training products; computer software and electronic databases developed by federal agencies; and technical reports prepared by research organizations worldwide.

For more information about NTIS, visit our Web site at <http://www.ntis.gov>.

# **NTIS**

**Ensuring Permanent, Easy Access to  
U.S. Government Information Assets**



U.S. DEPARTMENT OF COMMERCE  
Technology Administration  
National Technical Information Service  
Springfield, VA 22161 (703) 605-6000

---